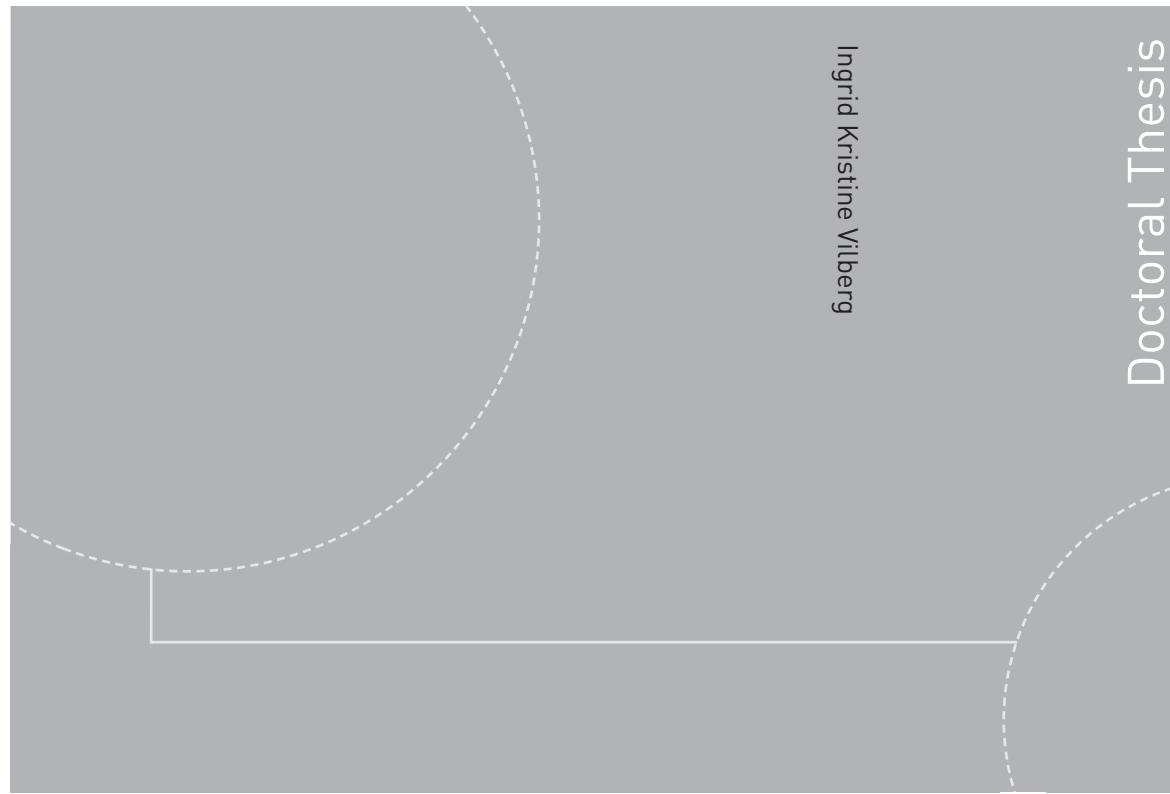


ISBN 978-82-326-3666-2 (printed version)
ISBN 978-82-326-3667-9 (electronic version)
ISSN 1503-8181



Ingrid Kristine Vilberg

Doctoral Thesis

Doctoral theses at NTNU, 2019:30

Ingrid Kristine Vilberg

**Study of cavitation, pressure
pulsations and flow control methods
in hydro power plants**

NTNU
Norwegian University of
Science and Technology
Faculty of Engineering
Department of Energy and Process Engineering

Doctoral theses at NTNU, 2019:30

NTNU

NTNU

Norwegian University of
Science and Technology

NTNU

Norwegian University of
Science and Technology

Ingrid Kristine Vilberg

Study of cavitation, pressure pulsations and flow control methods in hydro power plants

Thesis for the degree of Philosophiae Doctor

Trondheim, February 2019

Norwegian University of Science and Technology
Faculty of Engineering
Department of Energy and Process Engineering



Norwegian University of
Science and Technology

NTNU

Norwegian University of Science and Technology

Thesis for the degree of Philosophiae Doctor

Faculty of Engineering

Department of Energy and Process Engineering

© Ingrid Kristine Vilberg

ISBN 978-82-326-3666-2 (printed version)

ISBN 978-82-326-3667-9 (electronic version)

ISSN 1503-8181

Doctoral theses at NTNU, 2019:30



Printed by Skipnes Kommunikasjon as

Abstract

Hydro power plants play an important role in balancing power supply and maintaining a constant grid frequency. With the large water storage capacity, hydro power is in a favourable position with regard to operational flexibility to balance intermittent renewable energy sources, such as wind and solar power. Operation of Francis turbines outside the best efficiency point leads to draft tube pressure pulsations and cavitation, with unwanted effects like noise, vibration and erosion which cause increased wear and maintenance requirements.

Flow control is a collection of methods and technologies to modify flow conditions and achieve more favourable situations. Air injection in draft tubes is a common flow control method to attenuate pressure pulsations due to increased compression and reduced wave propagation velocity. These effects can also be favourable with regards to elastic waves in long pipe lines, pressure pulsations and water hammers. This thesis studies the use of flow control methods in hydro power plants, with emphasis on air injection. The presented work is focused around three main experiments.

The runner blades at Svorka power plant experienced cavitation erosion, and several measurements were carried out to identify the operational areas with the highest risk of erosive cavitation. By installing plexi-glass windows on the draft tube, we were able to visually correlate the erosion damages and the collapse of cavitation clouds.

The effect of a draft tube water injection system on pressure pulsations and cavitation was also studied at Svorka power plant. At installation, the injection system showed positive effects for mitigation of pressure pulsations. However, results from the study presented in this thesis indicate that the injection system has negligible effect on both cavitation and pressure pulsations. This could be due to the amount of air admitted through the runner shaft and variation in turbine submergence because of uncertainties regarding water level of the river and sedimentation in front of the outlet.

The effect of air injection was further investigated in a cavitation tunnel experiment, where the coupled effect between hydrofoil cavitation shedding and system dynamics of the

tunnel with various gas content was in focus. The results showed a correlation between shedding frequency and the pressure dynamics of the tunnel, but the shedding was not affected by the air content of the tunnel. Nevertheless, such a link might still exist and could possibly be detected by using a different experimental approach.

The aim of the last experiment was to assess the transient characteristics of a 1400 m pipe line to evaluate the wave propagation velocity and air content of the pipe. This was carried out by creating water hammers in the system. Furthermore, standing waves were created in the pipes by using a rotating valve apparatus to vary the pipe outlet area and impose periodical variations of flow rate and pressure. A more comprehensive and improved experiment will be planned based on the results and experiences from this study.

Collectively, these experiments show that the presence of gas can affect wave propagation velocity and elastic waves, if uniformly distributed. However, the gas can also accumulate in pockets and define a new dynamic element in the system. Gas injection can be used as a flow control method, but it should be taken into account that the gas can collect and create accumulators in the system which can improve or decrease system performance.

Preface

This project has been carried out at the Waterpower Laboratory, Department of Energy and Process Engineering at the Norwegian University of Science and Technology (NTNU) in Trondheim. Professor Torbjørn K. Nielsen has been the main supervisor and dr.ing Morten Kjeldsen in Flow Design Bureau AS (FDB) has been the co-supervisor.

This is an Industrial PhD project which is partly funded by my employer FDB and The Research Council of Norway (project number 248334/O30).

Acknowledgements

This work would not have been possible without the contribution from my supervisors, colleagues and collaborators. I would like to thank my supervisor Professor Torbjørn K. Nielsen for guidance throughout the project. Morten Kjeldsen has been the co-supervisor and the key contributor to this whole project. I would like to thank him for the opportunity to work on this research project, and for all support and inspiration essential for my progress.

I also express my gratitude to my colleagues in FDB, Håkon Francke, Jarle Vikør Ekanger and Andreas Tønnesen for their invaluable LabView and measurement skills and excellent cooperation during these years. Contributions from Xavier Escaler, from Universitat Politècnica de Catalunya in Barcelona, have been essential for the work on cavitation observation and measurements on Svorka power plant.

I would also like to thank Statkraft and Erik Wiborg for the possibility to use Svorka power plant for research purposes and for allowing us to install windows on the draft tube. Visual access to the draft tube in a prototype machine is unique and the studies have been both interesting and challenging.

Thanks to the Waterpower Laboratory for loan of the high-speed camera and light sources for the visual study, and to Rainpower and Kjell Sivertsen for cooperation on the second round of visual studies.

The great working environment at the Waterpower Laboratory has been an important motivation. I would like to thank all PhD-students and staff for great discussions and good times.

Last but not least, I am grateful for the support of my family and friends, and especially Mats. Thank you for the inspiration and understanding.

Contents

Abstract	i
Preface	iii
Acknowledgements	v
Contents	vii
Nomenclature	xi
Part I	1
1 Introduction	3
1.1 Objective	4
1.2 Research Overview	4
1.3 Outline of Thesis	6
2 Background	7
2.1 Francis Turbines	7
2.1.1 Draft tube pressure pulsations	8
2.2 Cavitation	8
2.2.1 Cavitation development	9
2.2.2 Cavitation in Hydraulic Machinery	11
2.3 Air content in water	13
2.3.1 Dissolved air	14
2.3.2 Bubbly flows	14
2.4 Flow Control	16
2.4.1 Flow Control Methods in Piping Systems	17
2.4.2 Flow Control Methods in Hydro Turbines	17
2.5 Previous Work in Research Group	19

3 Research Methods	21
3.1 Cavitation intensity measurements	21
3.1.1 Signal analysis	21
3.2 Hydrofoil cavitation analysis	22
3.3 Pressure frequency response	22
3.4 Visual studies	24
3.5 Simulations	24
4 Summary of Papers	27
4.1 Paper 1	27
4.2 Paper 2	28
4.3 Paper 3	29
4.4 Paper 4	29
5 Discussion	31
5.1 Ssvorka visual studies	31
5.2 SAFL cavitation tunnel experiment	32
5.3 IRIS pipe experiment	32
6 Conclusion	35
6.1 Ssvorka visual studies	35
6.2 SAFL cavitation tunnel experiment	36
6.3 IRIS pipe experiment	36
6.4 General conclusion	36
7 Further Work	39
References	41
A Background for Ssvorka Experiments	45
A.1 Introduction	45
A.2 Visual Experiments	46
A.2.1 Ssvorka Visual 1	46
A.2.2 Ssvorka Visual 2	48
Part II - Papers	49
Paper 1	51
Paper 2	59

Paper 3	69
Paper 4	79

Nomenclature

Symbol	Description	Unit
A	Cross-sectional area	[m^2]
C	Concentration of liquid	[mL_{gas}/L]
c	Wave propagation velocity	[m/s]
c	Absolute velocity	[m/s]
c	Chord length	[m]
c_L	Wave propagation velocity of the liquid	[m/s]
c_m	Axial velocity component	[m/s]
c_u	Tangential velocity component	[m/s]
f	Frequency	[Hz]
g	Gravitational acceleration	[m/s^2]
ΔH	Head rise	[m]
H_s	Submergence	[m]
h_{atm}	Atmospheric pressure	[mWC]
h_v	Vapor pressure	[mWC]
k	Polytropic exponent	—
k_H	Henry's laws constant	[M/atm]
l	Cavity length	[m]
P_{gas}	Partial pressure of gas	[atm]
p	Pressure	[Pa]
p_b	Internal bubble pressure	[Pa]
p_o	Local pressure at reference point	[Pa]
p_v	Vapour pressure of liquid	[Pa]
p_∞	Liquid pressure	[Pa]
ΔQ	Change of volumetric flow rate	[m^3/s]
R	Bubble radius	[m]

S	Surface tension	$[N/m]$
U	Velocity of fluid	$[m/s]$
u	Peripheral velocity	$[m/s]$
V_G	Volume of gas	$[m^3]$
V_L	Volume of liquid	$[m^3]$
w	Relative velocity	$[m/s]$
Z	Characteristic impedance	$[Ns/m^3]$

Greek symbols	Description	Unit
α	Angle of attack	[°]
α	Void fraction	—
ρ	Density	[kg/m ³]
ρ_G	Density of the gas	[kg/m ³]
ρ_L	Density of the liquid	[kg/m ³]
σ	Cavitation number	—
σ_i	Incipient cavitation number	—

Abbreviations

BEP	Best efficiency point
CFD	Computational fluid dynamics
DO	Dissolved oxygen
FDB	Flow Design Bureau AS
FM	FloMASTER
IRIS	International Research Institute of Stavanger
ITTC	International Towing Tank Committee
mWC	Meter water column
NPSH	Net positive suction head
NTNU	Norwegian University of Science and Technology
MOC	Method of Characteristics
RSI	Rotor stator interaction
RVR	Rotating vortex rope
SAFL	St Anthony Falls Laboratory
SLPM	Standard liters per minute
UMN	University of Minnesota

Part I

Chapter 1

Introduction

This thesis deals with hydro power and the use of flow control technologies. Hydro power is the most important energy source in Norway, where 96 % of the electric energy production is from hydro power. Norway is the sixth largest producer of hydroelectric energy in the world and the largest producer in Europe. The total capacity of Norwegian hydro power plants was 32 160 MW in 2013 and the total production was 134 TWh [1]. The Francis turbine is the most widely used turbine in Norway, as it is applicable to low-head power plants of 30 m up to high-head power plants of 700 m with a high efficiency [2]. The most recent power plant in Norway is Lysebotn II, which utilizes a head of 686 m with two Francis turbines of 185 MW each.

Hydro power plants play an important role in maintaining a stable energy supply and grid frequency, as the production from other energy sources like wind and solar power is more unpredictable. With the market's demand for flexibility and the increased amount of wind and solar power being integrated on the grid, the power plants must provide fast response to sudden changes in energy production and the turbine is hence operated more frequently outside its best efficiency point. Operation of the turbine at off-design conditions can cause unwanted effects like pressure pulsations from the draft tube swirl and cavitation with associated noise, vibration and erosion. The turbine will normally have a specific range where these unwanted effects are too dominant, and thus it will not be operated in this range.

Flow control is a collection of technologies used to manipulate flow conditions to achieve a more favourable situation. Some examples are reduction of skin friction drag, delay of boundary layer separation and enhance turbulence for mixing augmentation. The flow control methods can be active or passive, where the passive methods are permanent devices while the active methods require a control system and energy supply for activation.

In the hydro power industry the most commonly used flow control devices are passive methods for the draft tube flow. Pressure pulsations from the draft tube swirl for part load operation are the origin for pressure fluctuations in the conduit system and possible power swings, and flow control methods are applied to reduce the effects of the draft tube swirl. The use of air injection is a common method for dampening pressure pulsations by increasing the fluid compressibility and reducing the wave propagation velocity. Several flow control methods are presented in more detail in Chapter 2.

1.1 Objective

As mentioned above, hydro power plants play an important role in balancing power supply and maintaining a constant grid frequency. However, this flexibility requires more operation of Francis turbines outside the best efficiency point, which leads to draft tube pressure pulsations and cavitation with unwanted effects like noise, vibration and erosion that cause increased wear and maintenance requirements.

The main objective of this thesis has been to study flow control methods in Francis turbines and hydro power plants. This includes achieving improved simulation models and a better understanding of the existing flow control methods and instruments in use by FDB today.

This thesis includes the following research program:

- Study cavitation and pressure pulsations in a full-size Francis turbine with visual access.
- Investigate the effect of air injection on hydrofoil cavitation shedding and tunnel dynamics
- Review and investigate flow control methods on cavitation, pressure pulsations and pressure wave propagation

1.2 Research Overview

The research projects in this thesis comprise of both laboratory and field experiments combined with some simulations. The results are presented in the papers in Part II of this thesis, with a summary given in Chapter 4. The three main experiments are

- Svorka visual studies (March 2016 and February 2018)

- SAFL cavitation tunnel experiment (June 2015)
- IRIS pipe experiment (May 2017)

These experiments have resulted in four papers:

Paper 1 - Assessment of remote cavitation detection methods with flow visualization in a full-scale Francis turbine

X. Escaler, I.K. Vilberg, J.V. Ekanger, H.H. Francke, M. Kjeldsen

Published in Proceedings of the 10th International Symposium of Cavitation (CAV2018), Baltimore, USA, May 14-16, 2018.

The paper presents measurements and analysis of high speed video recordings from visual studies carried out at Ssvorka power plant. The draft tube was equipped with four plexi glass windows to obtain visual access of the turbine blade outlet cavitation. The observed cavitation was compared to the remotely measured cavitation intensity.

This paper was written by Escaler, who also carried out the analysis of the visual study. The measurements and visual experiment was conducted by the candidate, with Escaler and Kjeldsen's assistance.

Paper 2 - Influence of draft tube water injection system on cavitation behaviour in a full-scale Francis turbine with visual access

I.K. Vilberg, M. Kjeldsen, X. Escaler, J.V. Ekanger, T.K. Nielsen

Published in Proceedings of the 29th IAHR Symposium on Hydraulic Machinery and Systems, Kyoto, Japan, September 16-21, 2018.

This paper is also from studies at Ssvorka power plant. In addition to the visual studies, the effect of the installed draft tube water injection system on pressure pulsations and cavitation has been evaluated.

Paper 3 - The effect of gas content on cavitation shedding and test facility dynamics

I.K. Vilberg, M. Kjeldsen, R.E.A. Arndt, T.K. Nielsen

Published in Proceedings of the 10th International Symposium of Cavitation (CAV2018), Baltimore, USA, May 14-16, 2018.

This paper investigates the connection between cavitation shedding and the dynamic response of the cavitation tunnel with various gas content. The shedding dynamics of a cavitating hydrofoil was used as a excitation frequency and the pressure response was measured at different locations in the tunnel.

Paper 4 - Experimental assessment of pressure pulsations and transient characteristics of a 1400 m pipe line

I.K. Vilberg, M. Kjeldsen, B. Svingen, T.K. Nielsen

Published in Proceedings of the 13th International Conference on Pressure Surges, Bor-

deaux, France, November 14-16, 2018.

The large-scale experiments carried out on a 1400 m pipe line are presented in this paper. Several water hammer tests were carried out to evaluate the air content of the pipe. Furthermore, a valve apparatus with a rotating disk was used to change the outlet area of the pipe and thus imposing flow and pressure oscillations on the system.

1.3 Outline of Thesis

The thesis is divided into two parts, where Part I contains introduction to the research topics and background. Additionally, a summary of the experiments and research papers is given, with a discussion and conclusion of the results and recommendations for further work. The research papers are presented in Part II of the thesis.

Chapter 2

Background

An overview of the theoretical background of the topics in question is presented in this chapter.

2.1 Francis Turbines

The Francis turbine is the most commonly used turbine due to the wide area of application, ranging from low heads of 30 m to high heads of around 700 m. In the runner, pressure and dynamic energy from the water is converted into torque on the shaft. Furthermore, the water flows through the draft tube and out into the tail water. The draft tube cone is a diffuser to retrieve pressure energy from the runner outlet velocity by increasing the cross-sectional area. A challenge with Francis turbines is part load operation. The turbines are designed to operate around the best efficiency point (BEP), and operation at off-design conditions involves a lower efficiency, pressure pulsations and risk of cavitation. Pressure pulsations in Francis turbines typically arise from rotor stator interaction (RSI), where the runner blades pass through the wake of the guide vanes, and the draft tube vortex rope at part load operation. The frequency of the draft tube vortex rope, known as the Rheingans frequency, is around 0.2-0.4 of the runner rotational frequency [3]. The RSI induced frequencies depend on the number of runner blades and guide vanes.

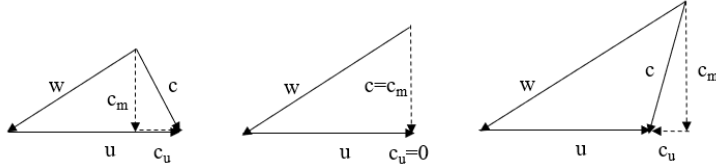


Figure 2.1: Velocity diagrams for runner outlet for a) part load, b) BEP with zero swirl and c) high load.

2.1.1 Draft tube pressure pulsations

The rotating vortex rope (RVR) in the draft tube originates from the tangential velocity component, c_u in the runner outlet as shown in 2.1. For operation at BEP the tangential velocity component is zero and the outlet flow is vertical. For part load operation the residual tangential velocity component will cause a swirl in the same direction as the runner rotation, while the opposite is the case for operation above BEP. The circumferential velocity u is constant, while the relative velocity w increases with increased load. c is the absolute velocity, with c_m and c_u as the axial and tangential component, respectively. The swirl number is the ratio between the tangential momentum and the axial momentum of the flow. A more detailed theoretical background of the draft tube flow can be found in Vekve [4] and Dörfler et al. [3].

In Rheingans' paper from 1940, he reported of power swings caused by draft tube pressure pulsations from the RVR which propagate upstream to the penstock. This cause a fluctuation in the effective head and thus the discharge, which lead to variations of torque on the runner and produce power swings [5]. Other consequences of part load operation are noise and vibration, which can ultimately lead to fatigue. Power plants are normally avoiding part load operation due to these effects to reduce maintenance costs.

2.2 Cavitation

Cavitation is defined as the formation of vapour bubbles in a liquid [6]. The inception, growth and collapse of vapour bubbles depend on the local absolute pressure in a flow. The cavitation number σ is given as

$$\sigma = \frac{p_o - p_v}{\frac{1}{2} \rho U^2} \quad (2.1)$$

Here p_o is the local pressure at the reference point, p_v is the vapour pressure of the liquid at the given temperature and $\frac{1}{2}\rho U^2$ is the dynamic pressure of the flow.

Cavitation occurs for low cavitation numbers, i.e. if the pressure at the reference point is decreased or if the dynamic pressure of the flow is increased by a higher velocity. Lowering the cavitation number further will increase the intensity of the cavitation, while a rise of pressure will reduce it [7]. The collapse of cavitation bubbles as they enter regions of higher pressure is a source of vibration, noise and pitting damage on adjacent material if the collapse near a surface.

2.2.1 Cavitation development

The development of a cavitation bubble is described in the following section, from inception to collapse.

Cavitation Inception

The cavitation number where cavitation is first detected is denoted the incipient cavitation number, σ_i .

Cavitation bubbles originate from small bubbles or nuclei in the fluid. The liquid-gas interface becomes unstable when exposed to a change in pressure and bubbles will grow rapidly when pressure is reduced. The onset of cavitation depends on the amount of cavitation nuclei in the liquid, i.e. small gas microbubbles in the liquid, gas trapped in small crevices on the material surfaces and organic impurities [8].

Once the bubble is formed, the growth and development depend on the difference between the interior bubble pressure and the liquid at the liquid-gas interface. At equilibrium, the following condition is satisfied at the interface [9]:

$$p_\infty = p_b - \frac{2S}{R} \quad (2.2)$$

Here p_∞ is the liquid pressure, p_b is the internal bubble pressure, S is the surface tension and R is the bubble radius.

The International Towing Tank Committee (ITTC) performed cavitation inception experiments using the same test body at several different test facilities. The results showed a large variation of the onset of cavitation due to content of cavitation nuclei in the liquid [10], [11]. Another study compared the cavitation shedding on NACA 0015 hydrofoils in

three different cavitaiton tunnels, and found that the shedding cycle appeared very different for the three facilities [12].

Growth and Development

The development of the vapour cavities can be classified in three main categories [13].

- Travelling bubbles
- Attached cavities
- Vortical cavitation

Travelling bubbles are formed in low pressure regions from small nuclei present in the liquid and carried along with the flow. They collapse when entering areas of higher pressure. This type of cavitation is strongly dependent on water quality i.e. air content and presence of micro-sized nuclei or bubbles in the liquid, but they are not as harmful with regard to erosion damages.

Attached cavitation form in the low pressure zone on a hydrofoil or blade and are attached to the solid wall. It is often denoted sheet cavitation when formed on a hydrofoil, and blade cavitation when occurring on pump or runner blades. This can be a very erosive type of cavitation, especially for attached cavities that are being shed and collapse as a could of bubbles in the proximity of a solid surface [14].

Vortical cavitation can occur from Von Karman vortexes which are being shed from for example a hydrofoil trailing edge or runner blade outlet, a tip vortex from a ship propeller or in the RVR in a turbine draft tube. The central core of the vortex has a low pressure where cavitation can develop. The vortex cavities are only erosive if they are in contact with a solid surface and the collapse occurs on the surface. The vortex shedding from hydrofoils or runner blades cause lift fluctuations with the same frequency as the shedding frequency, which can cause fatigue loads for frequencies close to the resonance frequency. The hydrofoil or runner blade trailing edge geometry can be modified to change amplitude and frequency of the shedding [2].

Collapse

A bubble collapse may result in high velocities, pressures and temperatures that can cause noise and material damage [14]. The collapse of a bubble generates local shock waves of high amplitudes and microjets in the fluid at the point of collapse. This causes high local

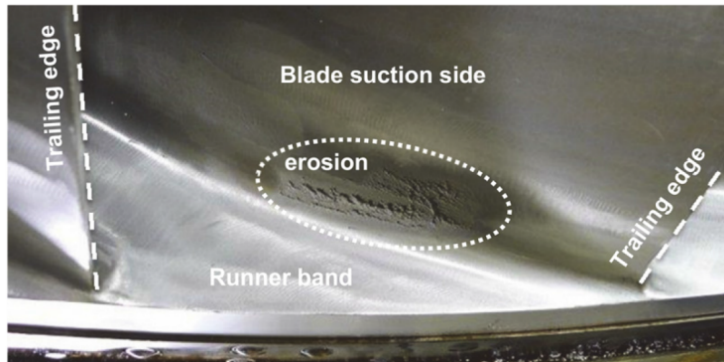


Figure 2.2: Cavitation erosion on runner blade at Svorka power plant [15].

stresses on solid surfaces close to the point of collapse. The typical erosion damage from cavitation on a pump or turbine blade is a sharp pit, while sediment erosion damages are much smoother.

2.2.2 Cavitation in Hydraulic Machinery

As can be seen from the cavitation number, cavitation can occur in areas of low pressure and high velocity in hydraulic machinery, typically in turbine outlets, pump inlets, pipe constrictions, valves etc. For hydro power turbines and pumps, the net positive suction head (NPSH) is an important factor for cavitation. The available suction head, $NPSH_A$, is given by the system parameters and the submergence level of the machine.

$$NPSH_A = -H_s + h_{atm} - h_v \quad (2.3)$$

Here H_s is the submergence of the machine, h_{atm} is the atmospheric pressure and h_v is the vapor pressure, all given in mWC. The available suction head must be larger than the required suction head to avoid cavitation. The required suction head, $NPSH_R$ depends on runner design parameters, like rotational speed, outlet angle and outlet velocity.

Visual access to a prototype machine is rare, as the visual studies are normally carried out during model tests. At Porjus power plant in northern Sweden, a 9.6 MW Kaplan turbine with a head of 60 m is dedicated to research and development activities. Visual studies with emphasis on cavitation were carried out on this unit [16].

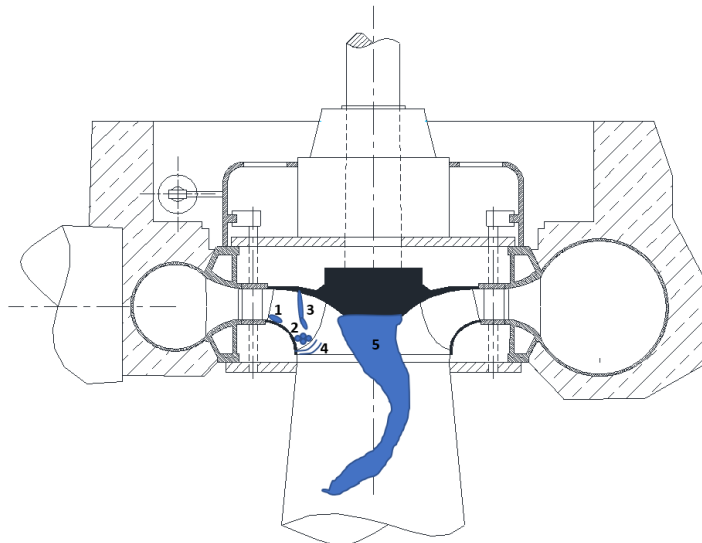


Figure 2.3: Cross-sectional view of Francis turbine showing the different types of cavitation.

Cavitation in Francis Turbines

Several parameters affect the development of cavitation in Francis turbines. Firstly, the runner dimensions are reduced in the design process to reduce costs, which cause a higher circumferential velocity of the runner and a lower cavitation number. The power plants also run more on part load operation, where the runner design is not optimized to avoid cavitation. Power plants with a large variation in available head will also be susceptible to cavitation problems due to regular operation at off-design conditions [17].

There are five main types of cavitation typically occurring in Francis turbines [17]:

1. Leading edge cavitation on runner blades

Leading edge cavitation can occur for operation with heads deviating from the design head, i.e. for hydro power plants with a large variation of reservoir level. For operation with a higher head than the design head, cavitation can occur on the suction side of the blade, while operation on a lower head than design head can cause cavitation on the pressure side. This type of cavitation may give rise to pressure pulsations and erosion on the runner blades.

2. Travelling bubble cavitation

Travelling bubble cavitation are bubbles originating from the blade suction side and can cause heavy erosion on the blade surface, as well as significant noise. This type of cavitation corresponds to operation with high local velocities in the runner, hence full load operation. It is dependent on the machine submergence and NPSH of the system.

3. Inter-blade vortex cavitation

Partial load operation may cause flow separation along the inlet edge and form a vortex between the runner blades. Inter-blade vortex cavitation will not give rise to significant erosion or vibration unless the cavitation vortex is in contact with the runner surface.

4. Trailing edge vortex cavitation

Cavitation bubbles formed as a vortex on the trailing edge of the runner blade will collapse further downstream in the draft tube where the pressure is increased. No serious cavitation erosion will occur when the bubble collapse is not in the proximity of any material. However, for cavitation occurring further upstream in the runner, a bubble collapse on the runner blade surface will cause erosion damage.

5. Draft tube swirl with a cavitating vortex core

The draft tube swirl is present below the runner cone at part load operation, rotating in the same direction as the runner. The rotational frequency is normally around 1/3 of the runner rotational speed, and is also known as the Rheingans frequency. Cavitation in the draft tube swirl does not cause erosion, but is the source of significant low frequency pressure pulsations causing strong noise and vibration in certain part load operational ranges. The low frequency pressure pulsations may also propagate upstream of the runner and cause power fluctuations.

Additionally, cavitation may occur in the gap between the shroud and the stationary lower cover, where the pressure is low and the peripheral velocity of the runner is high. Besides the mentioned erosion, cavitation may also be the source of dynamic loading on the runner blades. The shedding of sheet cavitation on the blades will give rise to lift oscillations which can cause fatigue issues.

2.3 Air content in water

Air can be present in water as small dispersed bubbles, often denoted as free gas, or dissolved in the liquid. The air may originate from brook intakes connected to the head race tunnel in hydro power plants. These intakes are characteristic because the small tunnel leading to the main tunnel will experience a free surface flow until a point where the tunnel is filled. In the zone where the jump from free surface flow to filled tunnel

occurs, there is a great possibility of free air to be mixed into the bulk liquid flow due to turbulence [18]. The process of air being mixed or dissolved in a liquid is known as aeration [19]. In a hydraulic jump, the aeration is driven by turbulence at the intersection of the free surfaces.

If assuming the air content originate from brook intakes of a power plant, there will be seasonal variations of the air content. A power plant will run significantly more on water from brook intakes during flooding and melting periods, normally during spring and autumn.

2.3.1 Dissolved air

Water can sustain a certain amount of gas in solution, which increases with pressure. The relation is given by Henry's law:

$$C = k_H \cdot P_{gas} \quad (2.4)$$

Here C is the concentration at saturation in the liquid, k_H is Henry's laws constant and P_{gas} is the partial pressure of the gas.

Dissolved gas is naturally present in water in a lake or a reservoir due to equilibrium at the free surface of the water and the atmosphere. Hydro power conduit systems have relatively high pressure further downstream, and gas is not susceptible to release. However, a non-stationary flow will lead to pressure fluctuations affecting the conditions for gas-release. The dissolved gas might be released in the case of repeated acoustical waves due to rectified diffusion. Rectified diffusion is a mass transfer in and out of a bubble, and the bubbles grow or dissolve under acoustic excitation [9]. Pressure fluctuations created by general turbulence can also be the driving force in rectified diffusion. Gas can also be released from solution in low-pressure regions, that could be created by swirls from mass flow fluctuations.

2.3.2 Bubbly flows

The presence of free gas in water will greatly affect the acoustic properties of the bulk liquid. Large cavities or air pockets will directly influence the total system characteristic by dampening and reflecting pressure waves, like air cushion chambers in hydro power plants. Free gas as small dispersed bubbles in a liquid will reduce the wave propagation velocity of the liquid, as will be demonstrated in the following.

For dispersed bubbles in a fluid, the gas content is described by the void fraction α .

$$\alpha = \frac{V_G}{V_G + V_L} \quad (2.5)$$

Here V_G is the volume of gas and V_L is the volume of liquid. The two-phase gas-liquid mixture has characteristic physical properties. While the density is close to that of the liquid, the compressibility is given by the compressibility of either the gas or the liquid [20]. The wave propagation velocity, c , in a flow with dispersed bubbles can be expressed as follows:

$$\frac{1}{c^2} = [\rho_L(1 - \alpha) + \rho_G\alpha] \left[\frac{\alpha}{kp} + \frac{(1 - \alpha)}{\rho_L c_L^2} \right] \quad (2.6)$$

Here ρ_L and ρ_G are the density of the liquid and gas phase, respectively, k is the polytropic exponent, p is the pressure and c_L is the wave propagation velocity of the liquid. To use this equation, one must assume an ideal gas behaving according to the polytropic equation $pV^k = constant$ [14].

The wave propagation velocity in water is around 1400 m/s, while it is approximately 340 m/s in air. As can be seen in Figure 2.4, the wave propagation velocity in an air-water mixture can be even lower than in air for relatively low void fractions.

Attenuation and scattering

Due to the compressibility of gas bubbles and the difference of impedance in the mixture, the presence of gas bubbles will reduce the amplitude of pressure transients in the flow. The amplitude is attenuated because of thermal, acoustic and friction damping in a cycle of compression and expansion of the bubbles [14].

A pressure wave will also be scattered when propagating between regions of different impedance. The impedance of a system is given as

$$Z = \rho \cdot c \quad (2.7)$$

where ρ is the fluid density and c is the wave propagation velocity. When entering a region of different impedance, the original pressure wave generates a reflected and a transmitted wave.

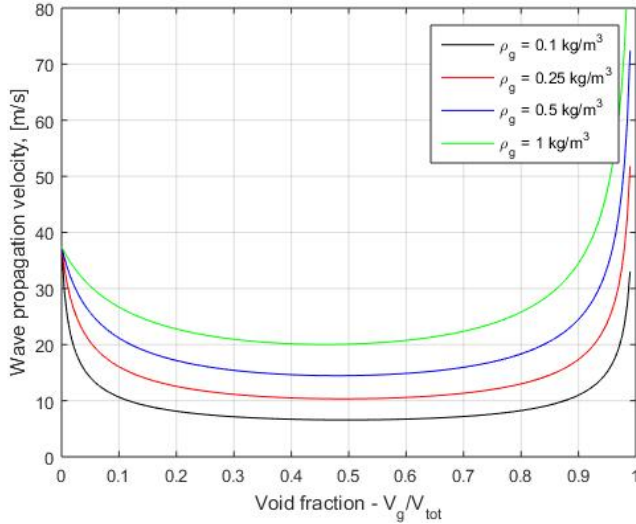


Figure 2.4: Wave propagation velocity as a function of void fraction.

2.4 Flow Control

Flow control is the use of various technologies to manipulate a flow to more favourable conditions [21]. Examples of common flow control technologies for industrial use are vortex generators on air plane wings to delay boundary layer separation and stall, and transition to turbulent boundary layer to enhance a mixing process. Some examples from nature are bumps on the fins of the hump back whale the rough riblets on shark skin that delay boundary layer separation [22].

The different flow control technologies are categorized in passive and active methods. Passive methods are permanent devices that do not require control or energy supply, like the previously mentioned vortex generators on air plane wings. Active flow control, on the other hand, require a control system and energy supply. The active control system can either be predetermined systems or reactive systems with a feed-back loop [21].

2.4.1 Flow Control Methods in Piping Systems

Drag reduction methods are common for long pipelines. Examples are delay of transition from laminar to turbulent boundary layer, control of boundary layer separation, surface coatings and addition of drag reducing agents [21]. For control of pressure transients in piping system, commonly used methods are air accumulators, like a closed air surge tank in hydro power plants, or a check valve to relief pressure.

Looking at the equation for head rise with a change of flow, $\Delta H = \frac{-c\Delta Q}{gA}$, it is evident that a reduction of the wave propagation velocity, c , can be effective. The wave propagation velocity depends on the elastic properties and geometry of the pipe, compressibility of the liquid and the gas-content of the liquid [23]. The elastic properties of the pipe may be altered by using a flexible hose. As previously mentioned, the compressibility of the liquid can be changed by adding air bubbles to the system. A French method from 1951 is to use a small flexible hose with air inside the pipe to reduce the effective bulk modulus of the system [24].

Although air injection is an effective method to mitigate pressure pulsations, it should be used with care. The air can accumulate and form larger pockets that introduces a new dynamic element to the system.

2.4.2 Flow Control Methods in Hydro Turbines

Flow control systems in Francis turbines are typically aimed at reducing pressure pulsations at part load operation. Several practical solutions are reviewed by Thicke [25], including structural additions to the draft tube like the use of fins and runner cone extensions. Although these permanent alterations might be beneficial at some narrow operational regimes, they have negative effects in other regimes closer to the BEP.

The use of fins in the draft tube was investigated experimentally by Nishi et al. [26]. The runner cone can be extended in different configurations, both by a stationary and a rotating extension. This was investigated experimentally by Vekve [4], Gogstad [27] among others, and numerically by Qian et al. [28]. With the cone extension, the originating point of the RVR is moved further downstream the draft tube which can reduce the strength of the RVR [4].

Furthermore, the use of air injection in the draft tube is a widely used method to reduce draft tube pressure pulsations. Air at atmospheric pressure is typically admitted through the runner hub to increase draft tube pressure, dampen pressure pulsations, reducing flow

noise and avoid an unsteady draft tube swirl. Air can also be admitted through the draft tube wall [29].

Air injection can also be used to reduce cavitation erosion, and studies have shown positive effects on both on hydrofoils and ship propellers [30]. In hydro turbines, air can be admitted upstream of the runner or directly on the runner blade surface [29], [31], but it is not commonly used.

Another application of air injection in hydro turbines is to increase levels of dissolved oxygen (DO) in the tail water [32]. Power plants with deep intakes can experience water with low DO which can be a risk to aquatic life in the tail water and the water must be aerated when passing the turbine [33].

Active methods

An active control method for Francis turbine operation stability was presented by Blommaert et al. [34]. They used a rotating valve exciter connected to the draft tube wall, which excited the draft tube with frequencies to cancel out the pressure fluctuation frequency. The system was tested experimentally and effectively reduced the pressure pulsations at a specific frequency.

A method for mitigation of the RVR was proposed by Resiga et al. [35]. As the other methods mentioned above aims at controlling the effects of the draft tube RVR, this method aims to address the main cause of excitation of the RVR. High pressure water is injected axially through the runner crown cone. The water jet aims to eliminate the stagnant central region below the crown cone, where the unsteady vortex rope is developed. The method was tested in a laboratory swirl rig and proved to mitigate the pressure amplitudes. The method has not been tested in a prototype machine. The jet method was further investigated numerically with different design modification for the jet injection by Rudolf et al., but the design modifications did not perform better than the original solution [36].

FDB has developed a draft tube injection system which injects high pressure water into the draft tube in opposite direction to the draft tube swirl. It has proven to reduce draft pressure pulsations and hence widening the operational range of the turbine [37]. The injection system has been installed at four power plants so far.

2.5 Previous Work in Research Group

Several previous studies relevant to this project have been carried out by FDB and our research partners dealing with cavitation, air injection and system dynamics, which form a foundation for the current project. Morten Kjeldsen, co-supervisor for this project and general manager in FDB, has experience in cavitation research from several projects and experiments both at NTNU and the University of Minnesota where he worked at St. Anthony Falls laboratory (SAFL) with Professor Roger Arndt. They studied the global dynamics of sheet and cloud cavitation, and the main findings were presented in Kjeldsen et al. [38] and Kjeldsen and Arndt [39]. The concept of test facility influence on cavitation studies was further addressed by Kjeldsen et al. [40].

Flow control technology has been one of FDB's main focus areas, mainly for the hydro power industry. A prototype draft tube injection system was developed by Kjeldsen and first installed at Skarsfjord power plant, owned by Troms Kraft. The injection system proved to be successful, and thus Håkon Francke started a PhD project developing and testing the injection system in a laboratory swirl rig and installing the second system on Skibotn power plant [41], also owned by Troms Kraft. Furthermore, an injection system was installed at Svorka power plant in 2010, where we also have installed plexi-glass windows for visual access and completed several cavitation detection experiments.

Further research on flow control methods was carried out during the author's Master's thesis in 2010, where the topic was the use of air injection to dampen pressure transients. FDB was also involved with Kjeldsen as a supervisor and Francke as a research advisor. Water hammer tests were carried out with air injection to reduce the amplitude and dampen the pressure transient [42].

The most recent contribution is the PhD thesis of FDB colleague Jarle Vikør Ekanger, investigating the relationship between variations of water quality and occurrence of cavitation in hydropower plants [43]. Ekanger carried out continuous cavitation intensity measurements at Svorka power plant and investigated the effect of water quality on cavitation. Water quality is influenced by particles and dissolved gas in the water, which was measured by turbidity meter. Ekanger also investigated this topic in a laboratory experiment at SAFL [44]. The development of cavitation detection analysis tools and LabVIEW programming was a central part of his project. These analysis tools have also been used in the experiments in the current thesis.

Chapter 3

Research Methods

The methods used for the three main experiments are presented in this chapter.

3.1 Cavitation intensity measurements

Cavitation intensity measurements and analysis were carried out in the experiments at Ssvorka. The remote measurements were conducted with high-frequency accelerometers and an acoustic emission sensor. Two accelerometers were placed on the turbine guide bearing and one accelerometer was placed on the guide vane shaft. The acoustic emission sensor was also placed on the turbine guide bearing. Additionally, the draft tube pressure was measured with three pressure sensors on the draft tube wall. The instrumentation is further described in Paper 1 and 2. Measurements were taken for certain operational points in the whole operating range of the turbine.

3.1.1 Signal analysis

The analysis process is based on previous studies at Ssvorka [15], [43]. The first step is to identify the frequency range of the power spectra where the signal levels are increased. To avoid noise from other sources, the highest possible frequency band should be in focus. Furthermore, the signal is band-passed filtered in this frequency range. The second step is to obtain the envelope function of the band-passed signal. By using a Hilbert transform, the envelope of the band-passed signal is obtained. By analyzing the frequency spectra

of the envelope function, the modulated frequencies are evident. Typical modulation frequencies originate from RSI, runner RPM and draft tube vortex surge.

There are different methods for estimating the power of the modulated frequencies, i.e. the cavitation intensity. One method for evaluating the power of the signal around the modulated frequency is to average a span with a certain amount of amplitudes around the relevant frequency in the demodulation spectrum. The span is decided based on the resolution of the spectrum. This approach has been used in the previous studies at Svorka [15]. To subtract the effect of the baseline noise level, it is possible to use the same approach on a nearby frequency.

The method used in this study, as presented in Paper 2, is to use the standard deviation of the signal in a narrow band pass around the modulation frequency. Here, wider frequency ranges were used for the baseline noise level.

3.2 Hydrofoil cavitation analysis

The parameter $\sigma/2\alpha$ is used to compare results for different values of the cavitation number, σ , for various angles of attack, α . The shedding frequency can be described by the composite parameter fl/U , where f is the frequency and U is the flow velocity. l is the observed maximum cavity length and is a function of $\sigma/2\alpha$.

In a previous study by Kjeldsen et al. [38], the cavitation regimes on a NACA 0015 hydrofoil were mapped for various cavitation numbers and angle of attacks. The results are shown in Figure 3.1. l/c is the ratio of the cavity length and the chord length, and this relation was also used for the shedding analysis in the experiment presented in Paper 3.

3.3 Pressure frequency response

In a frequency or pressure response analysis, the system in question is excited with a disturbance of constant frequency, and the pressure response is measured and analyzed in the frequency domain. The frequency is changed with small steps to ensure a sufficient resolution. For certain frequencies, the system will have an enhanced pressure response which determines the critical frequencies that lead to resonance in the system.

In the experiment at SAFL, the excitation frequency for the system was the shedding frequency of the cavitating hydrofoil. The shedding frequency was not controlled or constant, as for standard frequency response measurements. The excitation frequency for the

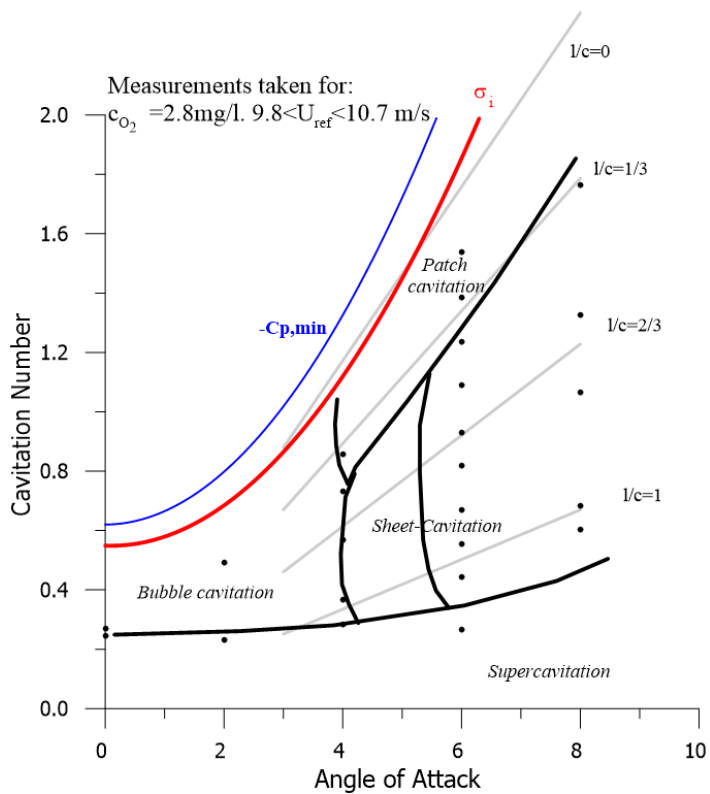


Figure 3.1: Cavitation regimes for a NACA 0015 hydrofoil [38].

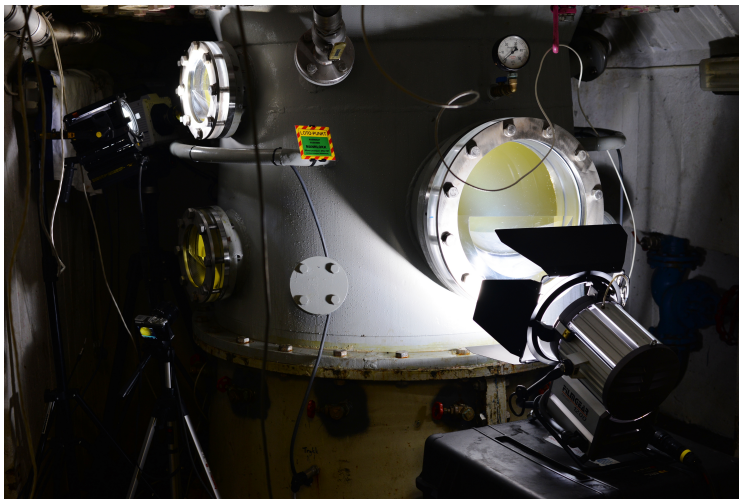


Figure 3.2: Set-up of lamps and cameras for visual studies at Svorka.

pipe at IRIS was controlled and held constant with the rotating valve apparatus which applied a varying outlet area of the pipe.

3.4 Visual studies

The first visual studies were carried out with a high-speed camera and high luminosity lamps which provided continuous lighting, as shown in Figure 3.2. Lamps were used in the man hole window and the top right of the smaller windows. The high-speed camera was placed in the top left window, behind the smaller lamp. In the second study, a camera synchronized with a stroboscopic light was used. The window view angle was altered before the second visual study, see details in Appendix A.

3.5 Simulations

The test facilities at SAFL and IRIS were both simulated in the commercial software FloMASTER [45], which is a 1D CFD program for modeling and analysis of piping systems. Simulations in FloMASTER are based on the Method of Characteristics (MOC), which

is described in Wylie and Streeter [23]. The partial differential equations for momentum and continuity are transformed into total differential equations by MOC. The air content of the pipes is not modelled directly in the simulations, but a calculated wave propagation velocity based on the assumed air content is set for each pipe segment. Only the components that are simulated with MOC require input of the wave propagation velocity. For the simulations of the pipes at IRIS given in Paper 4, the varying outlet area of the pipe was modelled using the scripting function in FloMASTER.

Chapter 4

Summary of Papers

A summary of the published papers is given in this chapter. Full length papers are included in Part II.

4.1 Paper 1

Assessment of remote cavitation detection methods with flow visualization in a full-scale Francis turbine

X. Escaler, I.K. Vilberg, J.V. Ekanger, H.H. Francke, M. Kjeldsen

Published in Proceedings of the 10th International Symposium of Cavitation (CAV2018), Baltimore, USA, May 14-16, 2018.

This paper describes the visual experiments and cavitation measurements carried out at Svorka power plant. Regular visual inspections of the runner revealed cavitation damages on the suction side of the blades. However, some blades were more damaged than others, so the main objectives of this analysis were to identify the operational range of the turbine where the erosive cavitation takes place and to investigate why only some blades are affected. Cavitation intensity measurements were carried out with high frequency accelerometers and an acoustic emission sensor. A high-speed camera was used for the visual study.

By analyzing the videos from the experiments, the collapse of cloud cavitation could be seen on the blade suction side corresponding to the location of the observed erosion. Although the air in the draft tube center made the visual studies rather challenging, the cloud cavitation could be observed from BEP to full load. The number of blades with cavita-

tion and the size of the cavities increase with increased operational load. The cavitation intensity measurements correspond to the visual observations, with growing cavitation intensity from BEP towards full load. The visual study also revealed that cloud cavitation indeed was only present at particular runner blades, which agrees with the observed cavitation erosion.

This paper was written by Escaler, who also carried out the analysis of the visual study. The measurements and visual experiment was conducted by the candidate, with Escaler and Kjeldsen's assistance.

4.2 Paper 2

Influence of draft tube water injection system on cavitation behaviour in a full-scale Francis turbine with visual access

I.K. Vilberg, M. Kjeldsen, X. Escaler, J.V. Ekanger, T.K.Nielsen

Published in Proceedings of the 29th IAHR Symposium on Hydraulic Machinery and Systems, Kyoto, Japan, September 16-21, 2018.

Paper 2 is also based on the visual studies carried out at Svorka power plant. The second visual study, Svorka Visual II, was carried out in cooperation with Rainpower. A stroboscopic light was synchronized with the shaft rotation and triggered the camera. In addition to the visual studies, the effect of the installed draft tube water injection system, both on pressure pulsations and cavitation, was analyzed in this experiment. Pressure was measured on the draft tube wall, and cavitation intensity measurements were performed as previously described.

When installed in 2010, the draft tube water injection system showed a successful reduction of draft tube pressure pulsations. As the injection system alter the draft tube flow conditions, it was interesting to investigate the effect on the measured cavitation intensity. However, the current results showed that the injection system had little effect on neither draft tube pressure pulsations nor the cavitation intensity. A reason for this could be the uncertainty and variation regarding the surface level of the river in the outlet, which has not been measured. A repeating problem at Svorka has been deposit of smaller rocks and sedimentation of the river at the draft tube outlet. These aspects will contribute to a variation of the machine submergence and hence the operating conditions of the water injection system and the air admission.

It was proposed to do another experiment with the air admission system completely closed off. Additionally, a long-term measurement campaign was initialized at Svorka power

plant. The effect of seasonal conditions on the measured cavitation intensity will be monitored, and the water level in the outlet will be measured continuously.

4.3 Paper 3

The effect of gas content on cavitation shedding and test facility dynamics

I.K. Vilberg, M. Kjeldsen, R.E.A. Arndt, T.K. Nielsen

Published in Proceedings of the 10th International Symposium of Cavitation (CAV2018), Baltimore, USA, May 14-16, 2018.

This paper presents the experimental investigation of the connection between cavitation shedding and the system response of the cavitation tunnel with various gas contents. The study was carried out in the cavitation tunnel at St. Anthony Falls Laboratory at the University of Minnesota. The tunnel was imposed with a excitation frequency from a cavitating NACA 0015 hydrofoil. The gas content of the tunnel was varied between degassed water, saturated water and continuous air injection downstream of the hydrofoil.

Pressure was measured at three locations in the water tunnel. The mounting base of the hydrofoil was equipped with three high-frequency accelerometers, for horizontal, vertical and axial acceleration. With the accelerometers, both low frequency lift and drag variations and high frequency cavitation were measured.

The results showed that there was a correlation between the shedding frequency and the dynamic pressure of the tunnel. However, the cavitation shedding dynamics did not seem to be affected by the gas content of the tunnel. That might be due to the effective gas collector tank which was placed directly upstream the test section, which could have removed most of the injected air. Additionally, the direct lift was not measured in this experiment. Only the vibration of the support base of the hydrofoil was measured, and was assumed to be representative for the lift oscillations.

4.4 Paper 4

Experimental assessment of pressure pulsations and transient characteristics of a 1400 m pipe line

I.K. Vilberg, M. Kjeldsen, B. Svingen, T.K. Nielsen

Published in Proceedings of the 13th International Conference on Pressure Surges, Bordeaux, France, November 14-16, 2018.

This large scale pipe experiment was carried out at the International Research Institute of Stavanger (IRIS). The test facility consisted of two parallel horizontal pipes with diameters of 7" and 5.5". The pipes were connected in one end with a 180° bend. At the other end, the 5.5" pipe was connected to a pumping system and the 7" pipe to an arrangement to connect different valves. Pressure was measured at eight locations along the pipe and the flow was measured downstream of the pumps.

The main objective for initial testing and assessment of the test facility was to evaluate the wave propagation velocity in the system and management of the air content of the pipe. This was done by using a manual ball valve at the 7" pipe outlet and imposing water hammers on the system. From these tests it was evident that a substantial amount of air was still present in the pipes, as the pressure wave was damped fairly quickly. Measures were taken to reduce the air content. Further water hammer tests showed that the air content was indeed reduced, but some air was still present. Furthermore, a rotating disk driven by a motor was installed at the pipe outlet, which varied the outlet area of the pipe and imposed a periodical variation of the flow rate and pressure.

The measured results revealed the fundamental frequency of the system, which was evident in both the water hammer experiments and the oscillating flow experiments. The amplitude response of the system was measured for a range of frequencies, and the third harmonic was found at approximately 2.1 times the fundamental frequency. Mode shapes of the measured values were compared to results from simulations. A more comprehensive and improved experiment will be planned based on the results and experiences from this study.

Chapter 5

Discussion

5.1 Ssvorka visual studies

The visual studies at Ssvorka gave valuable information of the type of cavitation giving rise to the erosion damages on the blades. However, when gaining visual access to the draft tube flow it was evident that the air admitted through the runner cone obstructed the visual access. When the turbine was operated further away from BEP, we had no visual access to the runner outlet. Unfortunately, it was not possible to shut off the air admission for the second visual study, as it would have been interesting to measure the effect of the air admission in addition to get better visual access. Furthermore, a temperature change overnight before the second study caused a discolouration of the water and made the visual studies impossible. This is further described in Appendix A.

With regard to the draft tube water injection system at Ssvorka, the effect is uncertain – especially related to the combined effect with the air admission. Measurements carried out directly after the installation showed that the injection system effectively damped pressure pulsations, as presented in Paper 2. Yet there was no effect of the injection system in the measurements conducted during this study. Another experiment without the air admission would also be beneficial in this regard, as the amount of air admitted might have been adjusted during the years. The amount of atmospheric air which is admitted to the draft tube is also dependent on the turbine submergence, which is affected by the water level in the outlet and the sediments and possible obstructions in front of the outlet. The water level of the river can and should be measured to improve the experiment, but the effect of the obstructions in front of the outlet is more difficult to quantify.

5.2 SAFL cavitation tunnel experiment

The system dynamics of a piping system also depends on the wave propagation velocity in the system, which was the basis for the experiment in the SAFL cavitation tunnel. The aim of the study was to investigate the link between tunnel dynamics and cavitation shedding at various wave propagation velocities, which was changed by varying the tunnel gas content. The cavitation shedding frequency of the hydrofoil was used as the excitation frequency for the system and the pressure response of the tunnel was measured.

The results showed that there was a correlation between the shedding frequency and the dynamic pressure response of the tunnel. However, the cavitation shedding dynamics did not seem to be affected by the gas content of the tunnel. There are uncertainties related to the effect of the stilling tank which was placed directly upstream the test section, which introduced an unknown dynamic element to the tunnel. Additionally, the lift on the hydrofoil was not measured directly, but the vibrations measured on the hydrofoil base was assumed to be representative for the lift oscillations. Another element of uncertainty in the experiment was that the hydrofoil shedding was both the source of the tunnel dynamics and the sink for measuring the effect of tunnel dynamics. It can be shown in a linear analysis, not including inertia, that the variation in shedding frequency is dependent on pressure and flow oscillations in the test section. The consequence of time dependent frequency affects the premise of a frequency response measurement, i.e. a constant frequency cavitation shedding or excitation source.

5.3 IRIS pipe experiment

A further study on using air injection to attenuate pressure transients was initiated on the IRIS test facility with a pipe of approximately 1400 m. This initial study was carried out to assess the transient characteristics of the pipes and develop methods for reducing the air content. As expected, the air content of the pipes proved to be a challenge for the experiment, but after several rounds of ventilation, flushing the pipes with a high flow rate and compression tests the air content was significantly reduced. This was evident in the water hammer tests. Standing elastic waves were created in the pipes using the rotating valve at various frequencies, and the pressure response of the system was enhanced around the fundamental frequency of the system. Experiences from this experiment were used for planning and improving the experimental setup and preparation before an air injection system will be tested and the effect on attenuation of the pressure waves will be measured.

In general, air injection in draft tubes is a well proven and common method to dampen

pressure pulsations. However, using air injection upstream of the runner to dampen pressure transients or water hammers have not been tested previously. This is the motivation for testing such an air injection system in the pipes at IRIS. It must be considered that the injected air may introduce a new dynamic element to the system if collected in pockets. Thus, small amounts of air should be injected to ensure a scattering of small bubbles, to achieve a brief change of wave propagation velocity thus attenuate pressure transients.

Chapter 6

Conclusion

The present thesis aimed to study cavitation and pressure pulsations in a full-size Francis turbine with visual access and investigate the effect of flow control methods on tunnel dynamics, cavitation and pressure pulsations. This was completed in three main experiments.

6.1 Ssvorka visual studies

The visual studies at Ssvorka power plant proved to be interesting and unique. We were able to correlate the cavitation erosion damages on the blade suction side to the observed collapse of cloud cavitation on the blades, even though the air admitted in the center was preventing visual access. Furthermore, the effect of the draft tube water injection system was uncertain in the current measurement, even though tests after installation showed a positive effect. With current knowledge and the observations made, one reason can be the amount of air admitted to the draft tube. There are also uncertainties regarding the water level in the river outlet and sediments and obstructions in front of the outlet.

It is generally challenging to carry out measurements at power plants due to time limitation, operational schedule and limited access. New and improved experiments might not be possible to carry out because of economical and operational aspects. Nevertheless, the two studies conducted at Ssvorka gave valuable information about the cavitation appearance and substantial experience in visual studies for actual hydro turbine installations.

6.2 SAFL cavitation tunnel experiment

The experiment at SAFL investigated the possible coupling between cavitation shedding and system response of the cavitation tunnel with different air content and thus various wave propagation velocity. In addition to being an important topic for research activities in closed-loop cavitation tunnels, it also provides a general insight in system dynamics.

The experiment indeed established that the shedding dynamics are present at all pressure measurement points in the loop. While injecting air, and thus modifying the wave propagation velocity, no or very limited effect was observed on the shedding amplitudes. The measured response also deviates from the calculated response. A possible explanation is that gas accumulates in parts of the loop and provides both attenuation of standing waves and optimal conditions for dynamic cavitation studies in the tunnel. As a conclusion, the cavitation shedding studies at SAFL seem to be little influenced by system dynamics. However, since closed loop tunnels are theoretically susceptible to system dynamics influence, this effect should be taken into account in other test facilities, especially for dynamic studies.

6.3 IRIS pipe experiment

The experiment on the IRIS pipe was an initial assessment of the facility and was successful with regard to evaluating the air content of the pipes and creating standing waves in the pipes. It will be used as a basis for further studies where an air injection system for mitigation of pressure waves will be tested.

6.4 General conclusion

To summarize, the main findings in this projects were:

- Correlation between erosion damages and the observed cavitation collapse in the visual studies at Svrkova power plant.
- Uncertainties regarding the effect of the draft tube water injection system in combination with the air admitted to the draft tube centre at Svrkova power plant.
- No correlation between the cavitation shedding and the variation in system dynamics of the system with regard to tunnel air content at SAFL.

- Established a procedure and basis for air removal, water hammer tests and generating standing waves in the system at IRIS, as a pre-study for testing flow control technologies.

For FDB this work has contributed to improved modelling and analysis abilities, as well as guidance for future development of flow control technologies based on the principle of gas in water.

With regard to the effect of gas in various flow systems, the presence of gas can, if uniformly distributed, affect wave propagation velocity and hence elastic waves. The same gas can accumulate in pockets and thus define a new dynamic element from a flow system perspective. The general conclusion is therefore that gas in water can be used as a flow control measure, but the accumulation of the gas can create dynamic elements or accumulators in the system. These accumulators can both improve system performance, like in the SAFL cavitation tunnel where boundary conditions were improved, or decrease the performance, as experienced with the negligible effect of the water injection system at Sverdlovsk power plant due to air injection.

Chapter 7

Further Work

The aim of this project was to evaluate the effect of flow control methods on cavitation and pressure pulsations in hydro power plants. The focus has been on the use of air and a final goal is to develop an active air injection system to mitigate pressure pulsations. This work continues and the present study provides the foundation on which further development will be made.

An apparent continuation of the visual studies at Svorka is another test where the air admission through the runner shaft is closed off. Then the effect of the air admission system and water injection system can be measured and the conditions for the visual studies will be greatly improved. Additionally, a commercial continuous cavitation measurement system was installed at Svorka power plant during 2018. To address the uncertainty of the water level in the outlet, a submerged pressure sensor has been installed in the outlet and the atmospheric pressure will be measured on the turbine floor. This measurement system will run continuously for years as a part of a more extensive monitoring system, which will also include sound monitoring. This will improve the understanding of two flow control approaches aiming to reduce the same effect, i.e. the Rheingans instabilities at part load operation.

To further investigate the correlation between cavitation shedding and tunnel dynamics, it might be beneficial to change the experimental setup. Instead of using the cavitation shedding as the source of tunnel dynamics, a controlled frequency excitation could be used. Nevertheless, to evaluate the coupling between system dynamics and especially the cavitation shedding frequency, a numerical 1D-3D coupled model should be developed. The 3D model includes the cavitating flow over the hydrofoil and the test section. Furthermore, the uncertainty of using vibration as a measure of the lift oscillations could be minimized by measuring the lift directly with load cells. By having both measurements,

the transfer function between the actual lift oscillations and vibrations at the mounting base could be evaluated.

Further work on the IRIS pipes includes a second and more comprehensive experiment for which the current study was used as an initial test and evaluation of the test facilities. The planned air injection system should be developed and tested in small scale to obtain a sufficient scattering of the bubbles, both in high and low velocity flows.

Bibliography

- [1] L.M. Hatlen and K. K. Arrestad. Fakta 2015: Energi- og Vannressurser i Norge. Technical report, Olje- og Energidepartementet, 2015.
- [2] H. Brekke. *Pumper & Turbiner*. Hydropower Laboratory, Norwegian University of Science and Technology, 2003.
- [3] P. Dörfler, M. Sick, and A. Coutu. *Flow-induced pulsation and vibration in hydroelectric machinery*. Springer, 2013.
- [4] T. Vekve. *An experimental investigation of draft tube flow*. PhD thesis, Norwegian University of Science and Technology, 2004.
- [5] W.J. Rheingans. Power swings in hydroelectric power plants. *ASME - Vol. 62 No. 3*, 1940.
- [6] R.E.A. Arndt. Cavitation in fluid machinery and hydraulic structures. *Annual Review of Fluid Mechanics*, 13(1):273–326, 1981.
- [7] F. R. Young. *Cavitation*. Imperial College Press, 1999.
- [8] D.H. Trevena. *Cavitation and tension in liquids*. Adam Higler, 1987.
- [9] J.P. Franc and J.M. Michel. *Fundamentals of Cavitation*. Kluwer Academic Publishers, 2004.
- [10] H. Lindgren and C.A. Johnsson. Cavitation inception on headforms, ITTC comparative experiments. *Proceedings of the 11th International Towing Tank Conference, Tokyo, Japan*, pages 219–232, 1966.
- [11] C.A. Johnsson. Cavitation inception on headforms, further tests. *Proceedings of the 12th International Towing Tank Conference, Rome, Italy*, pages 381–392, 1969.

BIBLIOGRAPHY

- [12] D. T. Kawakami, A. Fuji, Y. Tsujimoto, and R.E.A. Arndt. An assessment of the influence of environmental factors on cavitation instabilities. *Journal of Fluids Engineering*, 2008.
- [13] X. Escaler et al. Detection of cavitation in hydraulic turbines. *Mechanical Systems and Signal Processing*, 20:983–1007, 2006.
- [14] C. E. Brennen. *Cavitation and Bubble Dynamics*. Oxford University Press, 1995.
- [15] X. Escaler, J.V. Ekanger, et al. Detection of draft tube surge and erosive blade cavitation in a full-scale francis turbine. *Journal of Fluids Engineering*, 2015.
- [16] M. Grekula. *Cavitation Mechanisms Related to Erosion*. PhD thesis, Chalmers University of Technology, 2010.
- [17] S.C. Li. *Cavitation of Hydraulic Machinery*. London Imperial College Press, 2000.
- [18] A. Berg. Bekkeinntak på kraftverkstunneler. Technical report, Norges Hydrodynamiske Laboratorier, 1983.
- [19] H. Chanson. Hydraulics of aerated flows: qui pro quo? *Journal of Hydraulic Research*, 51, 2013.
- [20] V.E Nakoryakov, B.G. Pokusaev, and I.R. Shreiber. *Wave propagation in Gas-liquid media*. CRC Press, 1993.
- [21] M. Gad-el-Hak. *Flow Control*. Cambridge University Press, 2000.
- [22] D.M. Bushnell and K.J. Moore. Drag reduction in nature. *Annual Review of Fluid Mechanics*, 1991.
- [23] E.B. Wylie and V.L. Streeter. *Fluid Transients in Systems*. Prentice Hall, Inc, 1993.
- [24] G. Remenieras. Dispositif simple pour réduire la célérité des ondes élastiques dans les conduites en charge. *La Houille Blanche*, 1952.
- [25] R.H. Thicke. Practical solutions for draft tube instabilities. *Water Power & Dam Construction*, 1981.
- [26] M. Nishi, X Wang, K Yoshida, T Takahashi, and T. Tsukamoto. An experimental study on fins, their role in control of the draft tube surging. *Hydraulic Machinery and Cavitation*, 1996.

- [27] P.J. Gogstad. *Experimental investigation and mitigation of pressure pulsations in Francis turbines*. PhD thesis, Norwegian University of Science and Technology, 2017.
- [28] Z.D. Qian, W. Li, W.X. Huai, and Y. L. Wu. The effect of runner cone design on pressure oscillation characteristics in a Francis hydraulic turbine. *Proceedings of the Institution of Mechanical Engineers, Part A: Journal of Power and Energy*, 2011.
- [29] P.K. Dörfler. Design criteria for air admission systems in Francis turbines. *Proceedings of IAHR Symposium, Montreal, Canada*, 1986.
- [30] R.E.A. Arndt, C.R. Ellis, and S. Paul. Preliminary investigations of the use of air injection to mitigate cavitation erosion. *Journal of Fluids Engineering*, 1995.
- [31] A. Rivetti, M. Angulo, C. Lucino, and S. Liscia. Pressurized air injection in an axial hydro-turbine model for the mitigation of tip leakage cavitation. *Journal of Physics: Conference series*, 656, 2015.
- [32] B. Papillon, M. Sabourin, M. Couston, and C. Deschenes. Methods for air admission in hydroturbines. *Proceedings of the XXIst IAHR Symposium on Hydraulic Machinery and Systems, Lausanne, Switzerland*, 2002.
- [33] P. March. Hydraulic and environmental performance of aerating turbine technologies. *Proceedings of EPRI/DOE Conference on Environmentally-Enhanced Hydropower Turbines: Technical Papers, Palo Alto, California, USA*, 2011.
- [34] G. Blommaert, J.-E. Prenat, F. Avellan, and A. Boyer. Active control of Francis turbine operation stability. *Proceedings of the 3rd ASME/JSME Joint Fluids Engineering Conference, San Francisco, California, USA*, 1999.
- [35] R. Susan-Resiga, T. Vu, G.D. Ciocan, and B. Nennemann. Jet control of the draft tube vortex rope in Francis turbine at partial discharge. *Proceeding of the 23rd IAHR Symposium, Yokohama, Japan*, 2006.
- [36] P. Rudolf, J. Litera, G.A.I. Bolanos, and D. Stefan. Manipulation of the swirling flow instability in hydraulic turbine diffuser by different methods of water injection. *The European Physical Journal Conferences* 180(1):02090, 2018.
- [37] E.J. Wiborg and M. Kjeldsen. Francis at part-load with water injection. *Hydropower and Dams Asia*, 2012.
- [38] M. Kjeldsen, R.E.A. Arndt, and M. Effertz. Spectral characteristics of sheet/cloud cavitation. *Journal of Fluids Engineering*, 122(3):481–487, 2000.

BIBLIOGRAPHY

- [39] M. Kjeldsen and R.E.A. Arndt. Joint time frequency analysis techniques: A study of transitional dynamics in sheet/cloud cavitation. *Proceedings of the Fourth international symposium on cavitation (CAV 2001), Pasadena, California, USA*, 2001.
- [40] M. Kjeldsen, R. Vennatrø, R.E.A. Arndt, and A.P.Keller. Discussion on cyclic cavitation in closed water tunnels and the influence from the dynamic response of the tunnel. *IAHR Work group on the behavior of hydraulic machinery under steady oscillatory conditions, Brno, Czech Republic*, 1999.
- [41] H.H. Francke. *Increasing Hydro Turbine Operation Range and Efficiencies Using Water Injection in Draft Tubes*. PhD thesis, Norwegian University of Science and Technology, 2010.
- [42] I.K. Vilberg. Airbag for piping systems. Master's thesis, Norwegian University of Science and Technology, 2010.
- [43] J.V. Ekanger. *Investigation of the relationship between water quality variations and cavitation occurrence in power plants*. PhD thesis, Norwegian University of Science and Technology, 2016.
- [44] J.V. Ekanger. Cavitation intensity measured on a NACA 0015 hydrofoil with various gas content. *Proceedings of the 8th International Symposium of Cavitation, Singapore*, 2012.
- [45] Mentor Graphics. FloMASTER 8.1.
- [46] Statkraft. Svorka maintenance history. Technical report, 2015.

Appendix A

Background for Svorka Experiments

Several experiments and research projects have been carried out by FDB and collaborators at Svorka power plant. This section gives an overview of the previous projects and the studies conducted during this PhD-project. The papers related to this project are given in Part II, Paper 1 and 2.

A.1 Introduction

Svorka power plant is located in Surnadal in Møre and Romsdal county. It is owned by Svorka Energi AS and Statkraft AS, but operated by Statkraft. The dam and intake is in Måvatn, with a the maximum head of 260 m. The power plant has a head race tunnel of approximately 2500 meter, a surge shaft and penstock above ground. The maximum power is 25 MW with a flow rate of 11 m³/s. The machine is a vertical Francis turbine with 20 guide vanes and 15 runner blades, and the rotational speed is 600 rpm. The turbine discharges to river Bævra down-stream through a tunnel of approximately 20 m. The power plant was completed in 1963, but the runner was changed in 1998 [46].

The runner at Svorka suffered from aggressive cavitation erosion on the suction side of the runner blades, close to the trailing edge. According to the maintenance plan, visual inspections are conducted every two months and the runner is refurbished every five years [46].

Initial measurements of draft tube pressure pulsations were carried out by FDB at Svorka in 2009, and the results showed increased pressure pulsations at part load operation. Thus, it was decided to further develop and install a draft tube water injection system in coop-

eration with Statkraft. The installation was completed in 2010 and effectively reduced pressure pulsations, with the exception of operation at 12 MW where the pressure pulsations were increased with activation of the injection system [37].

The cavitation problems at Svorka were investigated further with FDB colleague Jarle Ekanger's cavitation intensity measurement campaigns from 2011-2014. The first cavitation intensity measurements were carried out at Svorka in 2011, in order to define the operational range with the highest risk of cavitation. The measurements were carried out in cooperation with Professor Xavier Escaler, using a similar measurement set-up as Escaler's previous experiments [13]. High frequency accelerometers and an acoustic emission sensor were placed on the turbine guide bearing. Additionally, accelerometers were mounted on the guide vane shaft and the draft tube wall. The results showed that the highest risk of cavitation was for maximum load [15], but due to lack of visual access it was not possible to evaluate the type of cavitation causing erosion on the suction side of the blades close to the trailing edge.

Following the initial cavitation intensity measurements, Ekanger set up a continuous cavitation intensity measurement system in addition to a turbidity probe and a DO probe for a measure of the water quality. The goal was to investigate the relationship between water quality and cavitation occurrence at Svorka. The monitoring system ran from May 2014 to January 2015, but due to some errors only data from May to August could be used for further analysis. The results were not conclusive, but did indicate an increased cavitation intensity with increased turbidity of the water [43]. The continuous monitoring system needed further development in terms of analysis and storing data, as the high frequency sensors provided an incredible amount of data.

Still lacking an answer to the type of cavitation causing the erosion on the runner blades, it was decided to modify the draft tube at Svorka and install windows to obtain visual access to the runner outlet and draft tube flow. In 2015 the draft tube was modified to fit three small acrylic windows in addition to a bigger window in the man hole. The windows would only be used for research purposes and blind flanges are used for normal operation of the power plant. The two visual experiments are described in the following sections.

A.2 Visual Experiments

A.2.1 Svorka Visual 1

The first visual study with the acrylic glass windows was carried out in March 2016 in cooperation with Xavier Escaler. We used a high-speed video camera to caption the

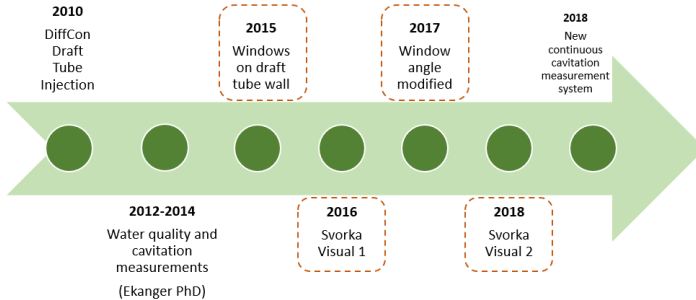


Figure A.1: Timeline of research projects on Ssvorka power plant. The highlighted projects are included in this thesis.

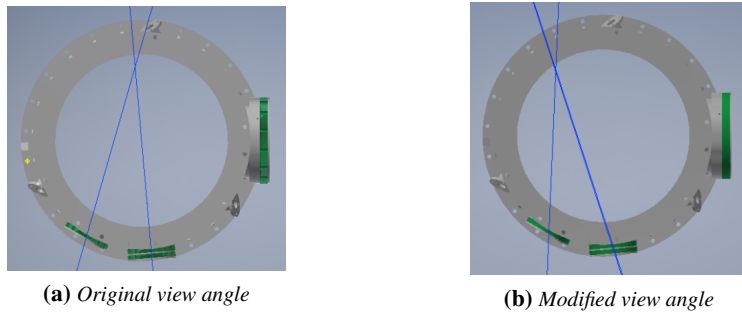


Figure A.2: Modification of view angle of windows

cavitation at the blade outlet. However, with visual access to the draft tube flow it was obvious that the air admitted in the center was obstructing most of the view of the blade outlet cavitation. By aiming the camera and lighting outside the air column, we were able to get some useful photos and videos in the operational range of 21-25 MW (85-100 %). Pressure and cavitation intensity measurements were conducted for the full operational range, both with and without the draft tube water injection system. Results from the visual study are presented in Paper 1 in and the results from tests on the draft tube injection system are given in Paper 2 in Part II. A summary of the results was given in Chapter 4.

A.2.2 Svorka Visual 2

An improved experiment was scheduled for February 2018. As the original view angle on the windows was directed through the draft tube center, it was decided to modify the view angle of the three smaller windows before the next experiment as shown in Figure A.2. The plan was also to shut off the air admission through the runner shaft to improve visual conditions in the draft tube and to measure the effect of air admission. According to manufacturing drawings, the air admission through the runner shaft could be regulated with a valve located in the runner cone, which could be reached from below. However, when this valve was inspected during the installation of the windows it became clear that another part was needed to close it. Unfortunately, it was not possible in our narrow time frame before the experiment. Thus, the experiment was carried out with air admission through the shaft, but the new view angle on the windows did improve the visual conditions to some extent.

The visual studies were carried out in cooperation with the Norwegian turbine manufacturer Rainpower. A stroboscopic light was synchronized with the shaft rotation, which also triggered the camera. The draft tube water injection system was not in operation during the experiments. The experiments were carried out during two days in February 2018. It was cold winter weather on the first day and the conditions for the visual studies were excellent with clear water. Unfortunately, the following day the water turned dark and dirty, which made the visual studies impossible. One possible reason for this is the significant temperature rise during night with rain and warmer weather. This may have caused discoloring of the water because of the humus from the march areas around the intake. Thus, only some photos from the first day were of adequate quality. The photos from this study are also presented in Paper 2.

Part II - Papers

Paper 1

Assessment of remote cavitation detection methods with flow visualization in a full-scale Francis turbine

X. Escaler, I.K. Vilberg, J.V. Ekanger, H.H. Francke, M. Kjeldsen

Published in Proceedings of the 10th International Symposium of Cavitation (CAV2018),
Baltimore, USA, May 14-16, 2018.

Assessment of Remote Cavitation Detection Methods with Flow Visualization in a Full Scale Francis Turbine

¹Xavier Escaler*, ²Ingrid K Vilberg; ³Jarle V Ekanger; ³Hakon H Francke; ³Morten Kjeldsen

¹Universitat Politècnica de Catalunya, Barcelona, Spain; ²Norwegian University of Science and Technology, Trondheim, Norway; ³Flow Design Bureau AS, Stavanger, Norway

Abstract

This paper describes the experimental investigations carried out in the Francis turbine at Svorka power plant operated by Statkraft in Norway. The unit, with a head of 260 m, can deliver a maximum output load of 25 MW. The rated flow rate is 11 m³/s and the machine rotates at 600 rpm. The turbine runner shows cavitation pitting on the suction side of the blades but some blades present more erosion than others. Moreover, preliminary studies based on remote monitoring of vibrations and acoustic emissions in this particular unit have predicted risk of erosion at high loads and the presence of a draft tube swirl affecting the cavity dynamics. In order to assess the sensitivity of these methods and the validity of the predictions, several acrylic-glass windows have been installed on the draft tube wall to visualize the runner outlet flow during operation. A high speed camera has been used to record the flow field during the tests with rates up to 5000 frames per second. A cavitation detection system has been installed comprising three high-frequency uniaxial integrated electronics piezoelectric (IEPE)-type accelerometers and an acoustic emission sensor, mounted in the turbine guide bearing pedestal and a guide vane arm. In particular, a series of measurements at different operation conditions have been carried out to correlate the simultaneous camera observations with the acceleration and acoustic emission overall levels in high frequency bands. The preliminary analysis of the camera records permits to certify the existence of erosive blade cavitation with the closure region close to the eroded areas at high loads. It can be seen that cavitation appears only in some blades and that it presents different cavity sizes for the same operation condition. As the load increases towards maximum powers, both the number of blades with cavitation and the size of the cavities grow. Moreover, the overall vibration levels also rise as expected.

Keywords: Francis turbine, cavitation erosion, high speed flow visualization, cavitation detection, vibration, acoustic emission

Introduction

Hydraulic turbine manufacturers and operators have to face with the drawbacks of suffering cavitation erosion when the units operate outside the best efficiency point. Currently, most of the machines require regular visual inspections to detect the extent of the erosion in order to replace the removed mass of material and to avoid a catastrophic failure. Obviously, this type of planned preventive maintenance is costly because it requires long machine shutdown. A most efficient procedure should be based on the predictive condition monitoring. For that, a remote measurement equipment is installed in the turbine and the adequate signal processing techniques are applied continuously without stopping the turbine.

In this direction, Flow Design Bureau AS is developing a cavitation erosion system to detect and predict the risk of erosion in hydraulic turbines with the help of UPC and NTNU. For that, a series of experiments have already been carried out in the Svorka power plant located near Surnadal in Norway. The plant is owned by Statkraft AS and Svorka Energi AS. The vertical shaft unit is a Francis turbine with a head of 260 m, rotating at 600 rpm and providing a maximum output power of about 25 MW. The runner has 15 blades and the wicket gate has 20 guide vanes. The turbine specific speed is 0.585 and the maximum turbine performance is reached around 21 MW.

This machine is of interest because it suffers aggressive erosion on the suction side of the runner blades close to the trailing edge as it can be seen in the photograph presented in figure 1. This type of erosion is caused by cloud cavitation detaching from the blade leading edge [1]. The methods used to predict cavitation are based on induced high frequency vibrations and acoustic emissions measured on the turbine guide bearing and the guide vanes [2].

*Corresponding Author, Xavier Escaler: xavier.escaler@upc.edu

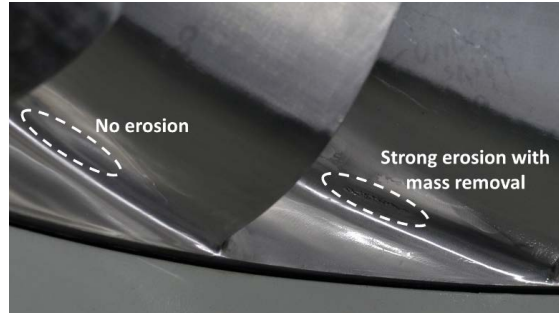


Figure 1. Photograph of the runner showing one blade with erosion and the contiguous one without erosion.

A preliminary investigation [3] has already demonstrated the feasibility of the installed measuring system and the applied signal processing techniques to monitor the activity of runner blade cavitation for unit operation above the best efficiency point (BEP). The results are consistent with the hypothesis that the highest risk of erosion would occur at full load. At this operating condition, the main hydrodynamic frequencies would force the shedding of cloud cavities, thus increasing their aggressiveness. Moreover, a draft tube instability modulating the runner blade cavitation dynamic behavior with periodic character has also been detected above BEP with maximum pressure pulsation levels at full load. Obviously, such detailed predictions could not be directly verified because the flow field inside the runner and draft tube cannot be observed in industrial environments such as any actual hydro power plant.

To the authors' knowledge and unfortunately, no literature reporting flow visualizations of blade cavitation in full scale prototypes can be found. Only in reduced scale model tests with transparent draft tube walls some limited research has been carried out to validate the cavitation remote monitoring techniques [4] which is not sufficient to validate the current methods in real machines. The typical design of the test rigs differs in many aspects from the full scale units. For instance, the signal transmission paths, the cavitation dynamic behavior and the level of aggressiveness might present significant differences that are not well known specially operating outside the BEP.

Consequently, it has been decided to design, construct and mount several transparent acrylic-glass (PMMA) windows around the draft tube wall that allow to visualize the cavitation flow exiting a Francis runner during operation. The final goal of the experimental investigation is to evaluate and validate the erosive cavitation remote measurements and procedures that permit to predict erosive cavitation and to estimate its aggressiveness.

Flow visualization setup

In order to have visual access to runner areas with detected cavitation erosion, three pipe-stubs were added to the draft tube into which 0.2 m diameter acrylic-glass bolts were fitted. In addition, a 0.42 m diameter acrylic-glass bolt was produced to replace the manhole cover. All the bolts surfaces were machined in such a fashion that allowed direct line-of-sight towards the erosion zones as indicated by the lines plotted in the outline presented on the left of figure 2. At the time of writing, the acrylic-glasses have been fitted twice in the pipe-stubs and the manhole. More specifically, they have been exposed to water between 2 and 3 days total, without presenting any observation of cracking or discoloration.

As it could be detected in a series of preliminary tests, the axis of the draft tube presents a gas-filled core for all the operation conditions as shown on the right of figure 3. The size of this cavitating vortex grows as the unit operates far from the BEP and obviously blocks the vision of the runner. Consequently, the camera had to be pointed away from the draft-tube center and given the current window positions the visible runner blades were observed when passing in front of the spiral casing end.

The high-speed camera used, model Photron® FASTCAM SA5, allows a frame-rate up to 7000 frames per second (f.p.s.) while still maintaining maximum resolution (1024x1024 pixels). During unit operation, the flow field was recorded with frame rates of 4000 and 5000 f.p.s., which correspond to a runner motion between frames of 0.9° and 0.72°, respectively, given the turbine rotating speed (10 Hz). As the field of view exceeds 24°, more than the angular separation between two consecutive blades could be recorded. The camera mounted a 50 mm f1.8 lens with the Nikon f-mount and it was focused on the blades eroded areas through one of the two smaller bolts located at the draft tube

*Corresponding Author, Xavier Escaler: xavier.escaler@upc.edu

top. Professional photographic lights were used that lighted through the manhole bolt and through the other smaller bolt located at the top.



Figure 2. (a) Outline of the acrylic-glass windows mounted on the draft tube with the adequate vision angle to see the blades; (b) photograph showing the flow visualization tests.



Figure 3. Vision of the runner from the manhole with the machine stopped (a) and with the machine operating at 19 MW (b).

Vibration and acoustic emission measurement

A cavitation detection system was installed that consisted of three high-frequency uniaxial integrated electronics piezoelectric (IEPE)-type accelerometers (AC) and an acoustic emission sensor (AE) mounted in the positions indicated in figure 4. Two of the accelerometers separated 90° , TGB1 and TGB2, were mounted on the turbine guide bearing pedestal using studs glued to its base that in turn screwed onto the sensor. Their axes were orientated in radial direction relative to the shaft axis. The other accelerometer, GV, was mounted at the top of a guide vane shaft using similar studs. Its axis was parallel to the shaft axis. The acoustic emission sensor, TGB, was also mounted on the guide bearing pedestal using a spring-loaded magnetic holder. Silicone grease was used between the sensor surface and the base surface. A preamplifier, supplied by a constant voltage source, was used to condition its signal.

All data recording was made using National Instruments (NI) hardware in conjunction with LabView® software. Signals were recorded using an NI cDAQ-9178 chassis. The accelerometers were conditioned and digitized using an NI 9234 IEPE module and the AE sensor using an NI 9215 AI [V] module. Accelerometer signals were recorded at 51200 samples per second (S/s) and the AE sensor at 250 kS/s. Several raw data time segments, each of 20 seconds duration, were recorded at each steady operation condition.

High speed observations and cavitation detection results

Based on the previous results [3] it was decided to concentrate the measurements and visual records in operating conditions ranging from the BEP (21 MW) up to full load (25 MW) in steps of 1 MW. The inspection of the runner blades just before the tests had shown that some blades were more eroded than the rest. In fact, only some blades presented strong mass removal and others did not show any significant mark. For example, such differences can be clearly seen in figure 1 where two consecutive blades are shown.

*Corresponding Author, Xavier Escaler: xavier.escaler@upc.edu

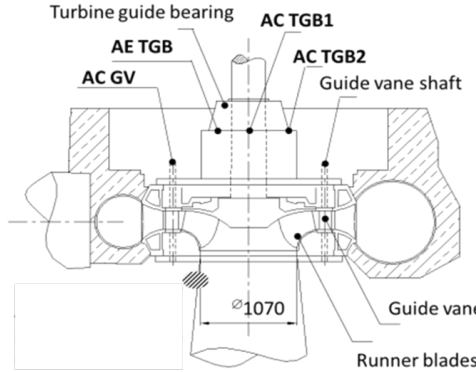


Figure 4. Location of the acceleration and acoustic emission sensors on the turbine guide bearing pedestal and guide vane shaft.

After analyzing the video records and identifying the 15 blades, it has been possible to compare their cavitation conditions among them for all the operation conditions. As it can be seen in figure 5, not all the blades present suction side cloud cavitation. For instance, blade number 6 appears not to suffer cavitation at all for any power output. On the contrary, blade number 14 is free of cavitation at BEP but develops cavitation for the rest of higher output loads. The global results regarding the presence of cloud cavitation for all the blades and operation conditions are summarized in table 1. Here it must be reminded that the field of view only corresponds to a narrow zone located next to the end of the spiral casing and no information about the evolution of the cavitation conditions as the runner blades span the whole circumference is available.

Firstly, it can be noted that only blade number 10 shows cavitation for all the loads including the BEP (21 MW). Then, cavitation starts at 22 MW for blades number 5, 13 and 14. At 24 MW, blades number 4, 6, 11 and 12 do not show cavitation yet. Operation condition at full load (25 MW) requires a special comment. Due to the significant increase of bubbles inside the flow, all the images appear excessively blurry and it is not possible to identify the presence of any type of large scale cavities. This unexpected behavior might be due to a deficient turbine setting point that reduces the available Net Positive Head (NPSHA) especially at full load.

	#1	#2	#3	#4	#5	#6	#7	#8	#9	#10	#11	#12	#13	#14	#15
21MW	-	-	-	-	-	-	-	-	-	Y	-	-	-	-	-
22MW	-	-	-	-	Y	-	-	-	-	Y	-	-	Y	Y	-
23MW	Y	-	-	-	Y	-	-	-	-	Y	-	-	Y	Y	-
24MW	Y	Y	Y	-	Y	-	Y	Y	Y	Y	-	-	Y	Y	Y
25MW	?	?	?	?	?	?	?	?	?	?	?	?	?	?	?

Table 1. Summary of the observations regarding the presence of blade suction side cavitation on all the 15 blades for operation conditions from 21MW up to full load at 25 MW. [Y] means that cavitation is detected, [-] means that it is not detected and [?] means that visualization information is not clear enough to distinguish its presence.

A more detailed observation of the flow field at 24 MW shown in figure 6 permits to clearly see the large-scale types of cavitation taking place when blades number 10 and 13 pass in front of the vision angle. As already commented, the closure region of the cloud cavitation on the blade suction side is observed as well as other forms of cavitation such as vortex shedding cavitation at the blade trailing edge and draft tube vortex rope cavitation from the runner hub. The overall RMS vibration acceleration and acoustic emission levels in the frequency bands from 18k to 20k Hz and from 95k to 97k Hz, respectively, have been plotted as a function of output load in figure 7. These results correspond to the average values from measurements taken in two different days. The data show that the levels increase with output load which corresponds to the increase of the number of blades with cavitation and the cavity sizes. The values in both guide bearing accelerometers are quite similar meanwhile the values in the guide vane are higher. The trends

from the two accelerometers and the acoustic emission sensor located on the guide bearing are analogous but the trend observed in the guide vane accelerometer differs slightly.

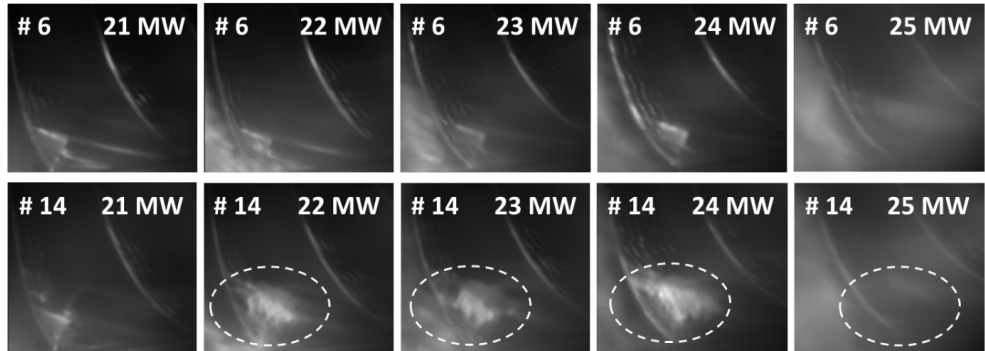


Figure 5. Flow visualization on blades number 6 (upper row) and number 14 (lower row) for operation conditions ranging from 21 MW up to full load at 25 MW. Suction side blade cavitation is observed for blade number 14 starting at 22 MW meanwhile blade number 6 does not exhibit cavitation at any operation condition.

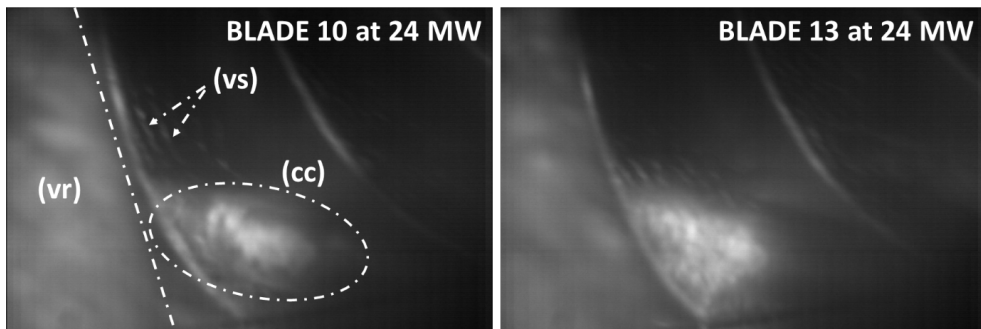


Figure 6. Zoomed view of the flow field at 24 MW when blades 10 (left) and 13 (right) pass in front of the vision angle that permits to identify cloud cavitation on the blade suction side (cc), vortex shedding cavitation at the blade trailing edge (vs) and draft tube vortex rope cavitation from the runner hub (vr).

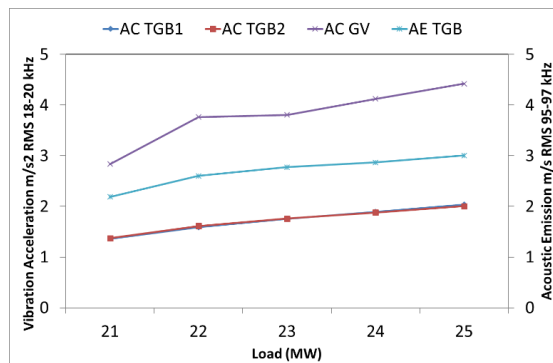


Figure 7. Overall RMS vibration acceleration and acoustic emission levels in the frequency bands [18k-20k Hz] and [95k-97k Hz] respectively, as a function of output load.

Conclusion

This work demonstrates the feasibility of installing visual access points on full-scale Francis turbine draft tubes to investigate cavitation phenomena inside the runner. The main objective is focused on answering at which turbine operation condition blade erosive cavitation takes place and how many runner blades are attacked. Analysis of video records taken with a high-speed camera has allowed identifying and quantifying runner cavitation from BEP up to full load. It has been observed that cloud cavitation on the blade suction side is responsible for the observed erosion. Surprisingly, cavitation is present in some blades even at BEP. As the load increases towards maximum powers, the number of blades with cavitation increases and the size of the cavities grows. Cloud cavitation seems to vanish at full load but it might be masked by the high bubble content of the main flow provoking images that are blurry. Based on overall measurements of cavitation erosion intensity obtained from induced noise and acoustic emissions with methods presented in previous works, a good correlation with the visual observations has been obtained. The remote cavitation measurements also suggest growing cavitation intensity from BEP towards full load, the latter with maximum aggressiveness, which is in agreement with the observations. Another significant confirmation is that the cavitation clouds are present only at selected runner blades, thus explaining the presence of erosion only at particular blades.

Acknowledgements

Ingrid K. Vilberg, an employee at Flow Design Bureau AS, is in parallel enrolled in the PhD program at NTNU. For this PhD related work, FDB receives partial funding from the Industrial PhD program at the Research Council of Norway and from the regional research funding program “RFF Vest”. PhD Bjørn W. Solemslie at NTNU provided initial guidance and “tips-and-tricks” for the use of the high speed camera.

Statkraft AS and Svorka Energi AS generously make the Svorka turbine unit available for research activities. In addition, services minded and dedicated staff at all levels within the two organizations contribute to the results achieved during testing. Statkraft’s Erik J. Wiborg is especially acknowledged for the fact that the visual access points were installed.

References

- [1] Avellan, F. (2004). *Introduction to cavitation in hydraulic machinery*. Proceedings of the 6th Int. Conf. on Hydraulic Machinery and Hydrodynamics, Timisoara, Romania.
- [2] Escaler, X., Egusquiza, E., Farhat, M., Avellan, F. and Coussirat, M. (2006). *Detection of cavitation in hydraulic turbines*. Mech. Syst. Signal Proc. 20(4).
- [3] Escaler, X., Ekanger, J. V., Francke, H. H., Kjeldsen, M. and Nielsen, T. K. (2015). *Detection of draft tube Surge and Erosive Blade Cavitation in a Full-Scale Francis Turbine*. J. Fluids Eng. 137(1).
- [4] Escaler, X., Farhat, M., Ausoni, P., Egusquiza, E. and Avellan, F. (2006). *Cavitation monitoring of hydroturbines: tests in a Francis turbine model*. Proceedings of the 6th Int. Symp. on Cavitation (CAV2006), Wageningen, The Netherlands.

Paper 2

Influence of draft tube water injection system on cavitation behaviour in a full-scale Francis turbine with visual access

I.K. Vilberg, M. Kjeldsen, X. Escaler, J.V. Ekanger, T.K.Nielsen

Published in Proceedings of the 29th IAHR Symposium on Hydraulic Machinery and Systems, Kyoto, Japan, September 16-21, 2018.

Influence of draft tube water injection system on cavitation behaviour in a full-scale Francis turbine with visual access

I K Vilberg^{1,2}, M Kjeldsen², X Escaler³, J V Ekanger², T K Nielsen¹

¹ Norwegian University of Science and Technology, Trondheim, Norway

² Flow Design Bureau AS, Stavanger, Norway

³ Universitat Politècnica de Catalunya, Barcelona, Spain

E-mail: ingrid.vilberg@fdb.no

Abstract. This paper describes the results of a comprehensive and ongoing project to control unsteady fluid-dynamic behaviour and associated effects at Svorka hydro power plant (25 MW, 260 m, 600 rpm), operated by Statkraft in Norway. This Francis unit had an original air admission system installed on the draft tube wall and turbine shaft. However, these systems did not perform satisfactorily to prevent high intensity pressure fluctuations due to vortex rope at part load. To mitigate them, a complementary draft tube water injection system, designed by Flow Design Bureau AS (FDB), was installed in 2010. Moreover, the runner suffered from cavitation pitting on the blades and a measuring campaign with several accelerometers and an acoustic emission sensor concluded that the unit was susceptible to high load cavitation erosion. Given the complexity of the turbine flow, it was decided to install four transparent acrylic glass windows on the draft tube, allowing for visual access to the runner blades and outlet flow. To evaluate the influence of the draft tube injection system on the cavitation behaviour, a series of measurements of cavitation intensity were carried out. High frequency data from the sensors were processed with demodulation techniques at various expected modulation frequencies, particularly the blade passing frequency and the frequency of the draft tube vortex rope. Furthermore, the pressure pulsations were measured and quantified with pressure sensors on the draft tube wall. The results indicate that draft tube water injection has little or no effect on the measured cavitation intensity in the runner. However, other aspects of the machine, including the seasonal and daily variation of the submergence level, must be taken into consideration. In conclusion, it appears that additional long-term observations are needed to clarify the global dynamic behaviour along the entire operating range.

1. Introduction

With the increased demand for flexibility in electricity production, Francis turbines are operated more outside the best efficiency point (BEP). Thus, off design operation leads to loss of efficiency and an increased risk of deleterious pressure pulsations and cavitation [1].

Pressure pulsations in the draft tube at part load operation are caused by the rotating vortex rope (RVR). The frequency of the draft tube pressure pulsations, known as the Rheingans frequency, is normally found between 0.2 and 0.4 times the runner rotational frequency [1]. Other pressure pulsations in Francis turbines are due to rotor-stator interaction (RSI); i.e. the interaction between the rotating runner blades and the stationary guide vanes.

Air admission in the draft tube is a common method to reduce pressure pulsations by dampening the high frequency components of noise and vibration [1]. Draft tube pressure pulsations can also be mitigated by injecting high pressure water jets tangentially into the draft tube in opposite direction to the draft tube swirl at part load operation [2], [3]. Flow Design Bureau AS (FDB) has designed several injection systems, including the one installed at Svorka power plant.

Svorka power plant consists of a single turbine unit with head $H=260$ m, rotating speed $n=600$ rpm and maximum output load $P=25$ MW. The turbine has 15 runner blades and 20 guide vanes. The unit has an original air admission system installed on the draft tube wall and turbine shaft, where ambient air is aspirated into the draft tube. A draft tube water injection system was installed in 2010, which consists of three injection nozzles. Upstream the injection nozzles, the pressure is controlled by a valve to allow an injection flow rate approaching roughly 1% of the nominal turbine flow rate at $P=25$ MW if draft tube pressure pulsation levels exceed pre-set thresholds when the turbine operates within pre-selected operation ranges. More specifically, the water injection system is automatically activated for part load operation for approximately 30-60 % of nominal power. Results from measurements after installation showed that the water injection system successfully reduced draft tube pressure pulsations at part load operation [3], as shown in Figure 2.

The runner at Svorka suffers cavitation erosion on the suction side of the blades close to the trailing edge, as shown in Figure 1, which may originate from cloud cavitation detaching from the leading edge [4]. Previous measurements on Svorka power plant, without draft tube water injection, had shown that the machine is prone to high load erosive blade cavitation and that the draft tube pressure pulsations propagate upstream the runner [5]. Hence, it was confirmed that the draft tube dynamics influenced the working conditions of the runner.

For research purposes, four acrylic glass windows were installed in the draft tube wall, as shown in Figure 3, to be able to visually inspect the cavitation during operation. A complete cavitation monitoring system was installed in order to correlate the obtained results with the actual cavitation conditions observed inside the runner and draft tube. Moreover, the effect of the draft tube injection system on the measured cavitation intensity was investigated and the injection system was operated manually in the full operating range of the turbine. During all the tests, air was admitted to the draft tube through the shaft and the draft tube wall.

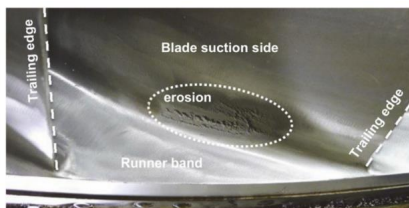


Figure 1. Cavitation erosion on blade close to trailing edge at Svorka runner.

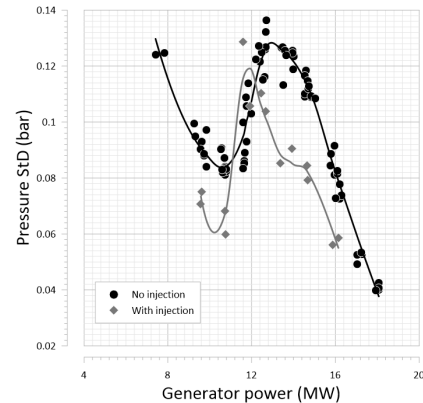


Figure 2. LOESS regression curves of draft tube pressure standard deviations showing the reduction of pulsations at installation of water injection system in 2010.

2. Experimental set-up

The experimental set-up was based on the previous measurements on Sorka reported by Escaler *et al.* [5] as shown in Figure 4. Accelerometers of the type B&K 4397A were placed radially and axially on the turbine guide bearing (AC TGB1 and 2) and on the guide vane shaft (AC GV). The acoustic emission sensor, Kistler AE - PC T5125, was located on the turbine guide bearing (AE TGB). Additionally, the penstock and draft tube pressures were registered with UNIK 5000 pressure sensors (PTX 5072-TA-A1-CA-H0-PA, industrial accuracy, 0-2.5 bar).



Figure 3. Draft tube at Sorka power plant with acrylic glass windows installed.

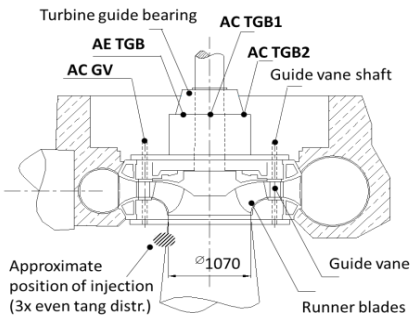


Figure 4. Cross-sectional sketch of turbine unit showing the position of sensors and draft tube injection system.

The signals were recorded using a National Instruments (NI) cDAQ 9184 chassis and LabVIEW software. The accelerometers were sampled at a frequency of 51.2 kHz and their outputs were recorded with a NI 9234 IEPE module. The acoustic emissions were measured with a NI 9205 module and sampled at 150 kHz. The pressure and guide vane opening signals were registered at a frequency of 1000 Hz with a second NI 9205 module with a $499\ \Omega$ resistance. At least two time segments of 20 seconds were recorded for approximately every steady operating point throughout the whole operating range of the unit from 1 up to 25 MW.

The visual observations were carried out with a GigE Vision Manta G-319 camera. Stroboscope lights were synchronized with the runner rotating speed and used to trigger the camera.

3. Signal processing

As in [5], the raw times signals were band-passed filtered between 20 and 25 kHz, and a Hilbert transform was applied to obtain the envelope functions. But in the current study, the modulation strength at the RSI frequency, $f_{RSI} = 200$ Hz, was determined by calculating the standard deviation, σ_{RSI} , of the bandpass filtered envelope function between $f_{RSI} \pm \Delta f$ with $\Delta f = 0.5$ Hz. Finally, the noise floor of the envelope function was subtracted to σ_{RSI} . This floor level was determined by using the same approach as for calculating σ_{RSI} but with frequency thresholds between 161-189 Hz and 211-239 Hz, and thus giving $\sigma_{Noise,L}$ and $\sigma_{Noise,H}$. As a result, the cavitation intensity level, I , was calculated as:

$$I = \sigma_{RSI} - \left(\frac{n_{s,RSI}}{n_{s,Noise}} \right)^{1/2} \cdot \frac{1}{2} (\sigma_{Noise,L} + \sigma_{Noise,H}) \quad (1)$$

where, $n_{S,RSI}$ and $n_{S,Noise}$ represent the number of spectral components contained within the bandpass thresholds used, i.e. $n_{S,RSI} = \frac{2 \cdot \Delta f}{1/t_s} + 1$, $n_{S,Noise} = \frac{189-161}{1/t_s} + 1 = \frac{239-211}{1/t_s} + 1$, where t_s is the sampling period, here typically 20 s.

4. Results

The visual observations confirmed that a considerable amount of air was admitted to the draft tube through the turbine shaft. As a result, a vortex column of air was present in the draft tube centre axis as shown in Figure 5 at all operating points, growing with operation outside the BEP. At part and full loads, the column of air extended almost to the draft tube wall and made visual studies close to impossible.



Figure 5. View of the runner and output flow through the man-hole window during operation (photograph by Statkraft).

Based on previous results predicting the risk of erosive blade cavitation at high load [5], visual studies were carried out from 19 MW up to maximum load. For all the operating points, von Karman vortex shedding from the blade trailing edges was observed. As full load was approached, it was possible to see cloud cavitation collapsing close to the eroded regions of some blades at their suction side. Clear images of erosive blade cavitation and of trailing edge vortex cavitation can be seen for output loads at 21 and 23 MW in the photographs shown in Figures 6 and 7. In Figure 6, the draft tube air vortex can also be seen.



Figure 6. Flow visualization at 23 MW showing von Karman vortex shedding, cloud cavitation and draft tube air vortex.

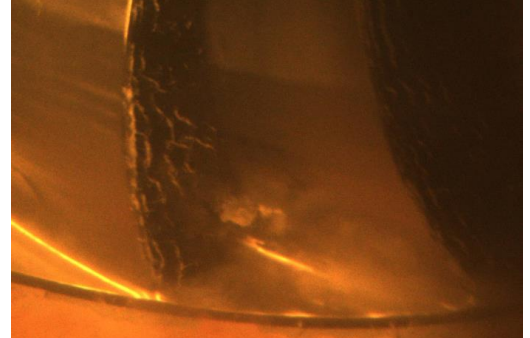


Figure 7. Flow visualization at 21 MW (photograph by Rainpower).

In Figure 8, the spectra of the draft tube pressure measurements without draft tube water injection show a distinct Rheingans frequency of around 2.4 Hz for part load operation, which is 24 % of the runner rotation frequency of 10 Hz. For higher loads above the BEP, a lower frequency of 0.4 Hz is also apparent. This frequency corresponds to the natural frequency of the elastic wave to the free surface in the surge chamber. In order to quantify the effect of the water injection system on the Reingans frequency, the standard deviations of the draft tube pressures in the band between 1.5 and 4 Hz are compared for measurements with and without water injection in Figure 9.

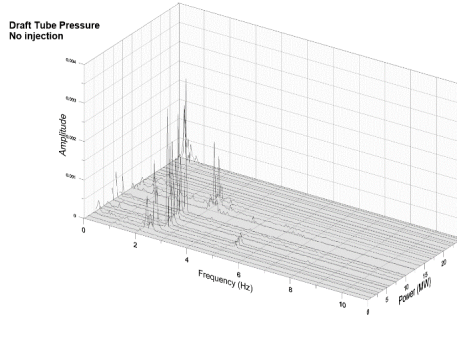


Figure 8. Spectra of draft tube pressure pulsations without water injection.

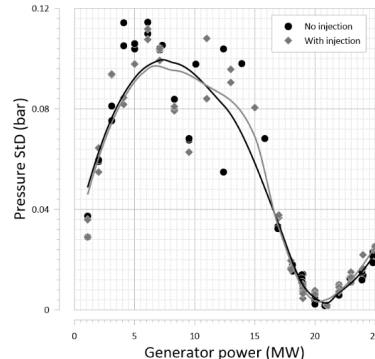


Figure 9. Standard deviations of draft tube pressures filtered between 1.5 and 4 Hz.

Figure 10 shows the amplitude modulation spectra from 0 to 250 Hz of the turbine guide bearing vibrations filtered in the band from 20 to 25 kHz for the full operating range with (left) and without (right) water injection. A clear peak is found around 0.4 to 0.6 Hz for high load operation. Conversely, there is no modulation peak around the Rheingans frequency for part load operation.

A modulation at the RSI frequency from a rotating point of reference, $f_{RSI} = 200$ Hz, can be seen at higher loads in all the accelerometers and the acoustic emission sensor, which corresponds to the guide vane passing frequency. Meanwhile, only the guide vane acceleration shows the RSI frequency from a stationary point of reference at 150 Hz. Amplitude modulations of turbine guide bearing accelerations

are shown in Figure 11 for frequencies from 195 to 205 Hz. It can be confirmed that f_{RSI} modulation is significant for higher loads, but it is not present at part load operation.

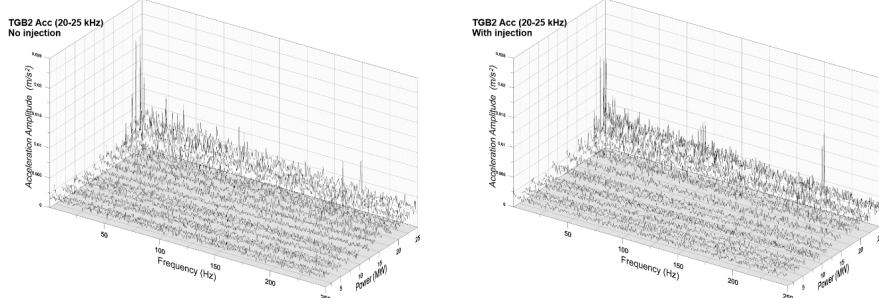


Figure 10. Amplitude modulation spectra of vibration acceleration at turbine guide bearing from 0 to 250 Hz.

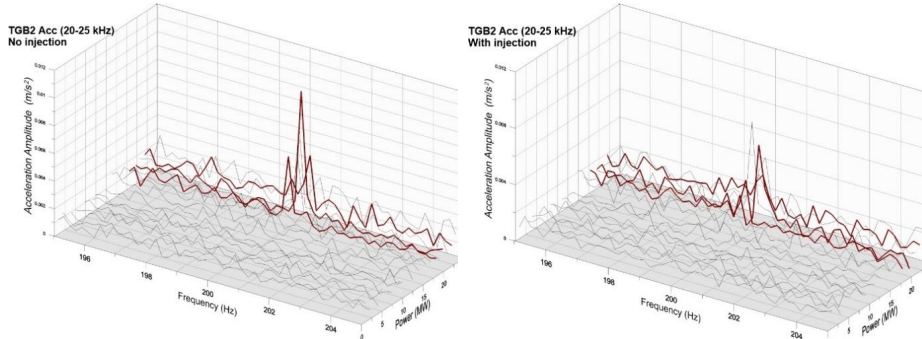


Figure 11. Amplitude modulation spectra from 195 to 205 Hz of turbine guide bearing acceleration. Highlighted lines correspond to operation points of 18, 20 and 22 MW.

The cavitation intensity level calculated from the turbine guide bearing vibration, I , is presented in Figure 12 for operation with and without water injection. The results indicate high cavitation intensity at high loads from 18 to 22 MW and at full load of 25 MW, with a minimum around 23 MW. Results from the rest of accelerometers show similar trends as already found in previous measurements [5].

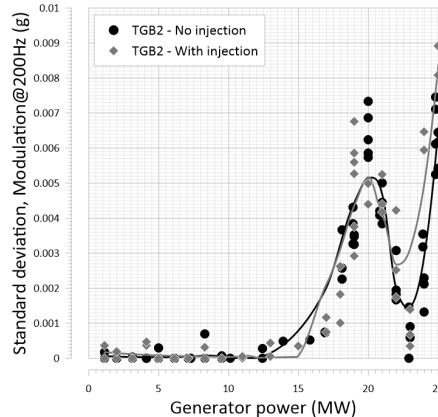


Figure 12. Cavitation intensity indicator based on standard deviations of turbine guide bearing accelerations (filtered from 20 to 25 kHz and modulated at 200 Hz) with and without water injection and LOESS regression curves.

5. Discussion

The air admitted through the turbine shaft made the visual studies very challenging. It formed a large air bubble in the draft tube centre which grew as the turbine was operated further away from BEP. Unfortunately, it was not possible to evaluate the total size and amount of air and how far downstream it extended. This large amount of air will obviously greatly affect the draft tube conditions by dampening pressure pulsations and modifying operational conditions.

Photographs of the runner showed von Karman vortex shedding from the runner trailing edges for most operating points with visual access not blocked by the central air column. These vortices are a sign of a poorly designed trailing edge and can contribute to a lower efficiency, but they are not a source of erosive cavitation. Cloud cavitation collapsing on the blade suction side close to the leading edge was also observed, which is responsible of the erosion. The number of runner blades with identified cavitation clouds increased with operating load, which is in agreement with the evolution of the cavitation intensity estimator and showing maximum values at high load operation.

It was demonstrated that modulation amplitudes at f_{RSI} of turbine guide bearing vibrations are slightly decreased when the injection system is operated, as shown in Figure 11. Similar trends could be seen for guide vane accelerations and acoustic emissions. However, the general noise level was increased for some areas of operation. This might be due to the fact that the injected water also suffers cavitation as it enters the draft tube. Evaluation of cavitation intensity by standard deviation values of band passed signals, Figure 12, showed that the injection system had little influence regarding the detected cavitation. However, the location of the peak amplitudes was shifted towards lower generator power levels, i.e. the high intensities measured at 20 MW are significantly reduced by injection, but the same levels appear at 18 MW.

The same tendency was found in the measured pressure pulsations at installation of the injection system, shown in Figure 2. The peak was shifted left towards lower powers. This was expected given the fact that water injection modifies the swirl of the draft tube flow [2]. This tendency is not evident for the current results presented in Figure 9. Now, the draft tube injection system does not appear to have the same effect on dampening the pressure pulsations as in the previous measurements. A possible reason for this is the uncertainty and variation regarding the surface level of the river, which has not been measured during neither the previous nor the current study. Another factor is the deposit of smaller rocks and sedimentation at the draft tube outlet. A variation in the submerge of the turbine will determine

the flow rate of air into the draft tube. It is believed that the effect of the water injection system will differ for various air admission flow rates.

6. Conclusion

The results obtained during tests of the Francis turbine at Svorka indicated that the draft tube water injection system had negligible effect on the measured cavitation intensity in the runner. After gaining visual access to the draft tube flow, it was evident that the air admitted through the runner shaft had to be taken into consideration to evaluate the water injection system performance. As well as being a source of uncertainty, the air in the centre of the draft tube made the visual studies more difficult and impossible at some operation conditions. Therefore, a repetition of the experiments presented here is suggested with the air admission system completely closed off. Furthermore, a long-term measurement campaign will be initialized at Svorka to monitor the effects of the seasonal conditions on cavitation intensity. In addition to the set-up of sensors described above, a continuous measurement of the water level in the outlet will also be included.

Acknowledgements

The topic of the current article is based on an unpublished article presented in Jarle V. Ekanger's PhD thesis [6], however the current study includes new measurements and analysis and more focus on the visual studies. The visual studies reported herein have been conducted in cooperation with the Norwegian turbine manufacturer Rainpower. Power plant operator Statkraft has facilitated the experiments, installed the draft tube injection system and allowed time for experimental work on the unit. The first author, Ingrid K. Vilberg is employed by FDB and enrolled in the Industrial PhD program by the Norwegian Research Council.

References

- [1] Dörfler P, Sick M and Couto A 2013 *Flow-Induced Pulsation and Vibration in Hydroelectric Machinery* (Springer)
- [2] Francke H H 2010 *Increasing hydro turbine operation range and efficiencies using water injection in draft tube* (Norwegian University of Science and Technology)
- [3] Wiborg E J and Kjeldsen M 2012 Francis at part load with water injection *Hydropower and Dams Asia*
- [4] Escaler X, Egusquiza E, Farhat M, Avellan F and Coussirat M 2006 Detection of cavitation in hydraulic turbines *Mechanical Systems and Signal Processing* **20** 983-1007
- [5] Escaler X, Ekanger J V, Francke H H, Kjeldsen M and Nielsen T K 2014 Detection of draft tube surge and erosive blade cavitation in a full-scale Francis turbine *Journal of Fluids Engineering* **137** 011103--9
- [6] Ekanger J V 2016 *Investigation of the relationship between water quality variations and cavitation occurrence in power plants* (Norwegian University of Science and Technology)

Paper 3

The effect of gas content on cavitation shedding and test facility dynamics

I.K. Vilberg, M. Kjeldsen, R.E.A. Arndt, T.K. Nielsen

Published in Proceedings of the 10th International Symposium of Cavitation (CAV2018),
Baltimore, USA, May 14-16, 2018.

The effect of gas content on cavitation shedding and test facility dynamics

^{1,2}Ingrid K. Vilberg *; ¹Morten Kjeldsen; ³Roger E.A. Arndt; ²Torbjørn K. Nielsen

¹*Flow Design Bureau AS, Stavanger, Norway;* ²*Norwegian University of Science and Technology, Trondheim, Norway,*

³*University of Minnesota, Minneapolis, MN, USA*

Abstract

This study investigates experimentally the coupling between cavitation shedding, considered as the source of tunnel dynamics, and the system response for various degrees of tunnel gas content. The experimental work took place in the high-speed water tunnel at the St. Anthony Falls Laboratory at the University of Minnesota. The test object was a c=81 mm NACA 0015 hydrofoil spanning the whole test section, 190mm by 190mm, at speeds around 10 m/s. Gas content was controlled by either comprehensive degassing, by allowing different gas saturations and eventually by continuously injecting air directly into the flow downstream of the test object. Most of the gas was removed by a gas collector, unique to the facility, upstream the test section. By combining simultaneous readings of pressure dynamics at three locations in the tunnel loop, together with measured shedding dynamic loads in parallel with high frequency impacts using the same externally mounted accelerometers, the research team aimed at concluding the effect of gas content on several cavitation characteristics. The results presented, and upon which discussion and conclusions are made, include excitation strength as a function of test section gas saturation level and the frequency response between the various pressure transducers and observed shedding strength.

Keywords: cavitation; hydrofoil; dynamics; cavitation tunnels

Introduction

The main benefit of using laboratory scale cavitation experiments is the relative ease of observing and documenting the underlying physics, and the ability of controlling all factors affecting the same physics. The International Towing Tank Conference (ITTC) demonstrated the lack of complete control for cavitation inception experiments, and observations on the same test-body at several facilities showed a wide scatter in results [1], [2]. The culprit of the observed discrepancy is often taken to be water quality, and most notably the tensile strength of the water in the test facility [3].

In 1997 one of the authors (MK) joined professor Arndt at St. Anthony Falls Laboratory (SAFL) at the University of Minnesota (UMN) to study the global dynamics of sheet and cloud cavitation, and the main findings were reported in Kjeldsen et al [4] and Kjeldsen and Arndt [5]. Based on observations in those studies the question was raised about the influence of the test facility on such studies. Following the SAFL studies and addressing the influence of test facility, Arndt repeated with co-workers many of the SAFL studies both at the Technical University of Munich /Obernach and University of Osaka, see Arndt [6] for a summary. Qualitatively the dynamics of cavitation shedding appears similar, as would be expected from the underlying cavitation physics, but with differences in measured unsteady lift amplitudes. Such differences can be attributed the response of the test facility, which is a line of investigation that has been addressed by e.g. Duttweiler et al. [7] and Kjeldsen et al. [8]. Other inspiration for the current work, but not necessarily including the role of system dynamics, stem from research on the role of water quality and gas content on cavitation intensity [9], as well as investigations into the shedding similarity between gaseous and natural cavitation [10]. This study tries to bring these efforts to a conclusion by modifying the one parameter that easily can be changed in the test facility: the sonic speed. This was accomplished by injecting gas downstream the cavitating hydrofoil, and thus modifying acoustic properties within most of the tunnel loop. The experimental program took place in 2015 at the SAFL high speed water tunnel.

*Corresponding Author, Ingrid K. Vilberg: iv@fdb.no

The interaction between cavitation and general system dynamics is not limited to laboratory testing. Large scale flow systems, such as hydropower plants, experience a wide variety of dynamic oscillations that can affect and interact with local cavitation phenomena and possibly induce extra loads on structures.

Experimental test facility

An overview of the high-speed water tunnel at SAFL is shown in Figure 1. The same figure illustrates the position of the absolute pressure transducers used to capture facility loop dynamics. The permanent instrumentation of the tunnel provided pressure and velocity measurements. Extracting water at the elbow downstream the test section and through a DO meter vessel, established the dissolved oxygen content. The air injection port, positioned shortly downstream the foil, allowed for continuous injection controlled and measured by an airflow controller. All experiments use the NACA 0015 hydrofoil, $c=81\text{mm}$ and span = 190mm, built in brass and polished. The foil being a cantilever construction attached to a rigid support base. On the latter three accelerometers (BK 4397) are mounted as shown in Figure 2, all being able to sense both low frequency lift and drag oscillations and high frequency cavitation intensity.

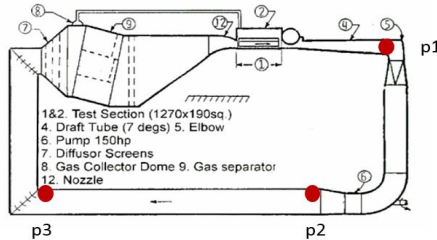


Figure 1: The cavitation tunnel at SAFL with indication for locations of dynamic pressure transducers.

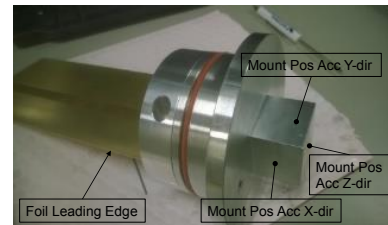


Figure 2: Test object, NACA0015, mounted on supporting base and with indications for location of high-frequency accelerometers.

Experimental observations

The measurements cited herein did not include direct measurements of lift. Instead the accelerometers attached to the base provide this information. There will be a frequency dependent transfer function associated to the determination of oscillating shedding loads using the accelerometers, but the experiment does not include a controlled frequency response experiment. Figure 3 compares the current experiment with results from a similar experiment carried out at Obernach in 1999, where the lift was measured directly. The obvious difference is the apparent higher amplitudes of oscillations for higher values of $\sigma/2\alpha$ when measured by the accelerometers (SAFL 2015), than by direct dynamic lift (Obernach 1999). The latter reading corresponds however qualitatively with other methods used for quantifying lift dynamics at SAFL.

Given the intention of the current study, focus is given the $\sigma/2\alpha$ range between 5.5 and 6.5, and for investigating the medium to high frequency range of 50-90 Hz. All SAFL 2015 studies are made at 8 degrees angle of attack. In addition, the $\sigma/2\alpha$ range was explored using velocities, U , in the range 7-10.5 m/s, and four different tunnel water qualities: 1) Degassed water with a low measured dissolved oxygen content, 2) high measured dissolved oxygen content, 3) continuous air injection of 10 slpm (standard liters per minute) and 4) continuous air injection of 20 slpm. The air injection point was at the tunnel test section wall approximately two chord lengths downstream the foil trailing edge.

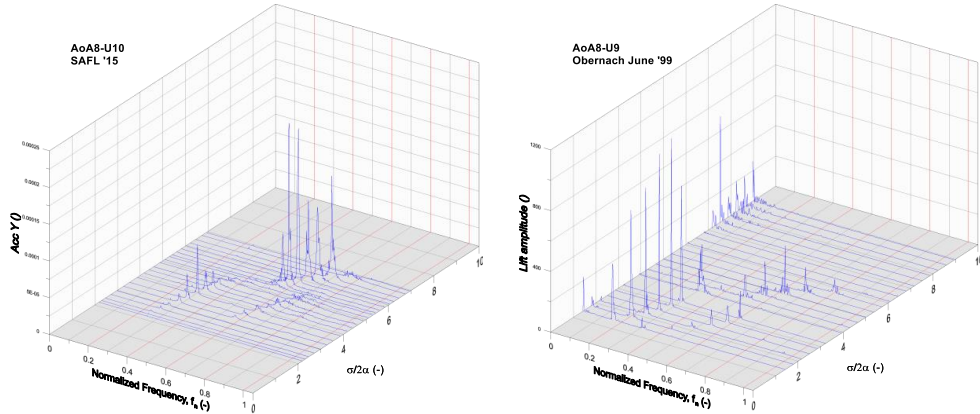


Figure 3: Comparison between SAFL2015 (left) and Obernach1999 (right) experiments, using accelerometers and direct dynamic load cells respectively, for the determination of lift oscillations on a cavitating NACA0015 hydrofoil.

Determination of excitation loads

One of the main objectives of the current study relates to the interaction between cavitation shedding physics and the systems. From the system perspective, the cavitation shedding defines the excitation and is characterized by its amplitude and frequency. Figure 4 shows the observed amplitudes and frequencies captured by the lift-direction mounted accelerometer. It appears that the normalized amplitude can be expressed as a function of frequency alone, both for different test section velocities and tunnel water qualities. The amplitude level has been calculated as the sum

of spectral components, $A = \sum_{i=n}^m a_i$ in a manually determined frequency range $\langle f_n, f_m \rangle$ containing the cavitation

shedding information. The shedding frequency is now calculated as $f_{cen} = A^{-1} \sum_{i=n}^m f_i \cdot a_i$.

Characteristics of excitation dynamics

Kjeldsen and Arndt describe the shedding frequency using the composite parameter fl/U [4]. Here l is the observed maximum cavity length and is a function of $\sigma/2\alpha$. Figure 5 shows the results from a visual determination of cavity length. A linear relation between cavity length is said to exist, and by using a type of expression as shown by Eq.1. Furthermore, fl/U is said to be constant within given $\sigma/2\alpha$ ranges. This allows the estimation of the l/c relationship based on measured shedding frequencies using e.g. the method of least squares on Eq.2 with data as given in Figure 4. Table 1 shows the results of this exercise, and Figure 5 shows the resulting l/c estimates compared with visually observed l/c data. The visual observation made my one of the authors (MK) in 1998.

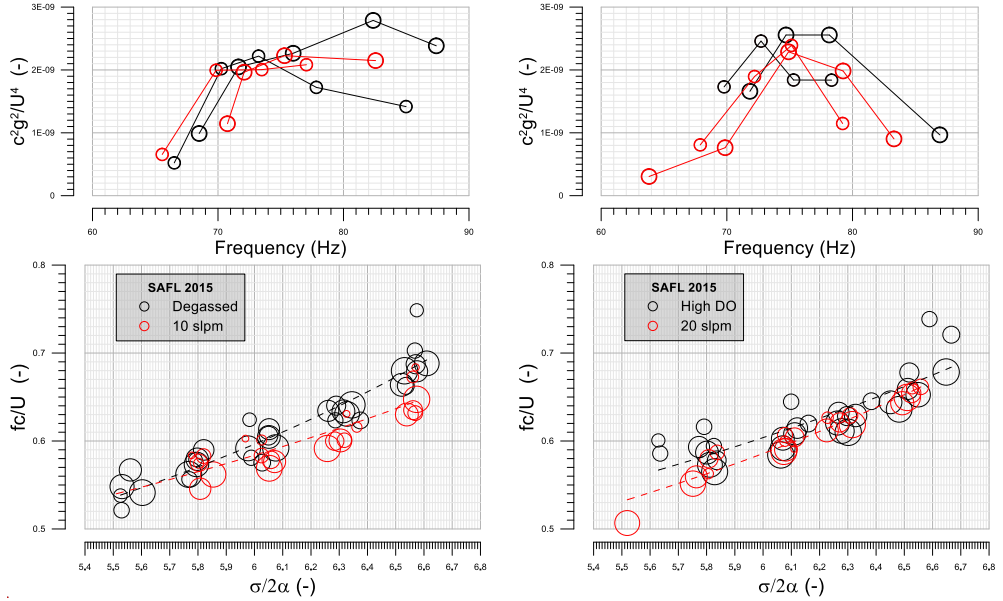


Figure 4: Cavitation shedding amplitudes (above) and frequencies (below). Amplitudes shown for two speeds, $U=10$ and 10.5 m/s the latter using slightly larger symbols, while the size of the symbols indicate velocities from 7 to 10.5 m/s using increasingly sized symbols. Dashed line indicates best estimates for $fc/U=\text{constant}$.

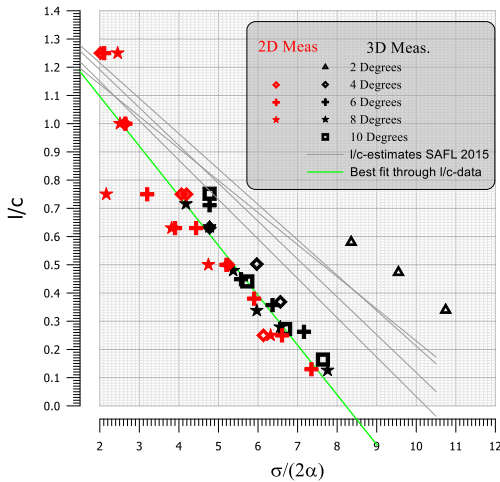


Figure 5: Maximum cavity extension length on a NACA0015 hydrofoil.

$$\frac{l}{c} = C_1 - C_2 \frac{\sigma}{2\alpha} \quad \text{Eq. 1}$$

$$\frac{fl}{U} = C_0 \Leftrightarrow \frac{fc}{U} = C_0 \left(C_1 - C_2 \frac{\sigma}{2\alpha} \right)^{-1} \quad \text{Eq. 2}$$

Quality	C_0	C_1	C_2
Degassed	0.367	1.429	0.1396
High DO	0.431	1.466	0.1253
10 slpm	0.400	1.367	0.1137
20 slpm	0.383	1.459	0.1341

Table 1: Estimates of cavity length relation based on observed shedding dynamics.

Observed system dynamics

Figure 6 shows cross-power spectra that indicate that the frequency content associated with shedding is present at the position of the dynamic pressure sensors. The cross-power spectra originate from the same set of data used for the spectrum of Figure 3. These plots reveal a more pronounced correlation at higher values of $\sigma/2\alpha$ and hence for higher frequencies. Based on this observation the SAFL 2015 study focuses on the cavitation shedding dynamics in the $\sigma/2\alpha$ range 5.5 - 6.5. The absolute frequency levels also allow more than one whole acoustic wave to be contained in the tunnel: $f=a/\lambda$ gives $f=33$ and 40 Hz for $a=1000$ and 1200 m/s, while assuming the wave length (λ) to be similar the tunnel loop length of approximately 30 m.

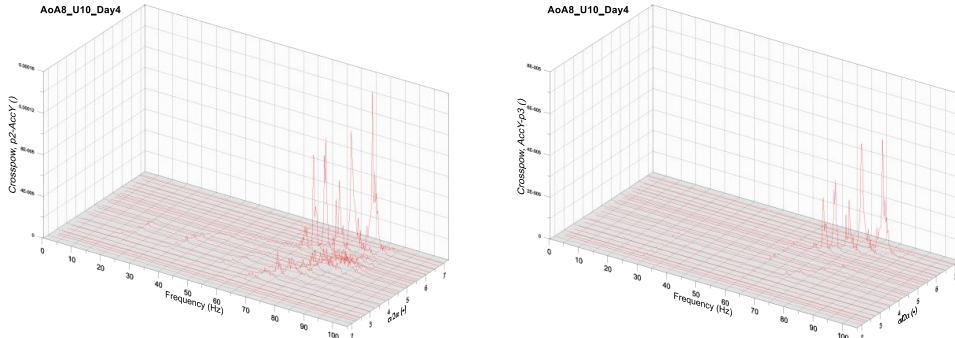


Figure 6: Cross power spectrum between lift-direction accelerometer and the two sensors at the lower leg of the tunnel (p2 and p3).

System modeling

The effect of the tunnel system dynamics on cavitation was evaluated using the time-domain solver, FloMASTER from Mentor Graphics. The software solves 1D transient flow problems using the Method of Characteristics (MOC). A time step of $dt=10^{-4}$ seconds was used for all calculations, allowing to resolve the smaller pipe segments, $L=0.6$ m, using MOC. Figure 7 shows the FloMASTER network used to model the SAFL cavitation tunnel. In addition to system layout, the required input includes sonic speed in the different pipe segments and modeling of the cavitation shedding excitation. These inputs are described more detailed in the following section.

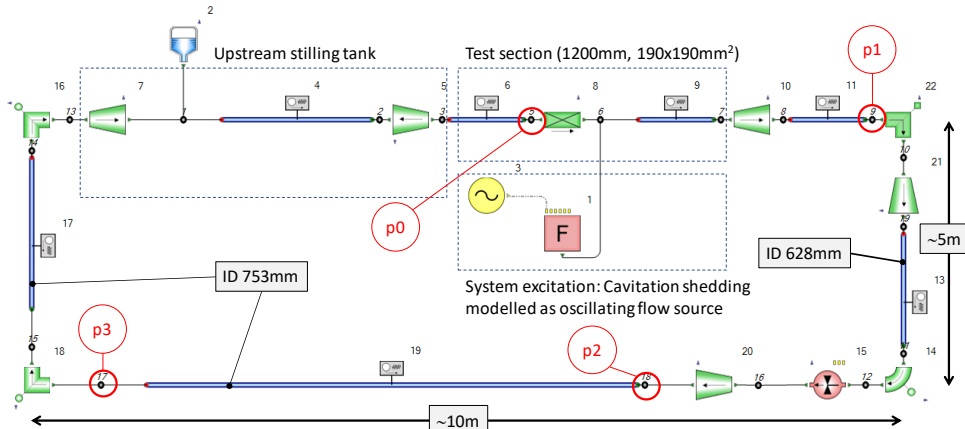


Figure 7: SAFL cavitation tunnel modelled in the software FloMASTER from Mentor Graphics. Pressures measured experimentally at locations p1, p2 and p3. Results from calculations include pressure response at position upstream the hydrofoil (p0).

Hydrofoil-dynamics

The hydrofoil cavitation dynamics can, in a first approach, be described using continuity and momentum equations as stated below.

1. Continuity over the hydrofoil: $U_2 A_{CS} = U_1 A_{CS} - \frac{dV_{Cav}}{dt}$, where the cavity volume (V_{Cav}) is a function of $\sigma/2\alpha$. A_{CS} is the cross-sectional area of the test section.
2. Momentum: Pressure loss over the element: $\Delta(p_1 - p_2) \cdot A \approx \frac{\partial F}{\partial C_D} \cdot \Delta C_D + \frac{\partial F}{\partial U_1} \cdot \Delta U_1$, i.e. the pressure difference is dependent on the drag coefficient C_D , which is a function of $\sigma/2\alpha$, and the speed of flow upstream the hydrofoil.

For system analysis, the cavitation shedding affects the cavity volume. In the system modeling this effect is included as an oscillating flow source, element 1. The drag coefficient, as given in the momentum equation, is included as a stationary resistance in element 8. The effect of the system is now determined by investigating the response in the pressure directly upstream the hydrofoil, node 5. A variation in this pressure should impact the hydrofoil cavitation shedding, and hence the degree of steady-oscillatory behavior.

Sonic speed of gas/liquid mixture pipes

The sonic speed of gas-water mixture can be calculated using Eq.3. Figure 8 shows the dependency of the mixture sonic speed on the gas void fraction (γ). For the flow loop the gas void fraction within the different pipes is defined as: $\gamma = Q_{Gas}/Q_{Tot}$. The gas volumetric flow rate also depends on the absolute pressures of the pipe, that is $Q_{Gas,Pipe} = Q_{Gas,0}(p_0/p_{pipe})$. For the current analysis $Q_{Gas,0}$ refers to the measured air injection flow rates which is taken at $p_0 = p_{atm}$. The pipe pressure is taken as the average between inlet and outlet. Table 2 gives an indication in the variation in sonic speeds for the lower leg as a function of operating conditions (U and $\sigma/2\alpha$).

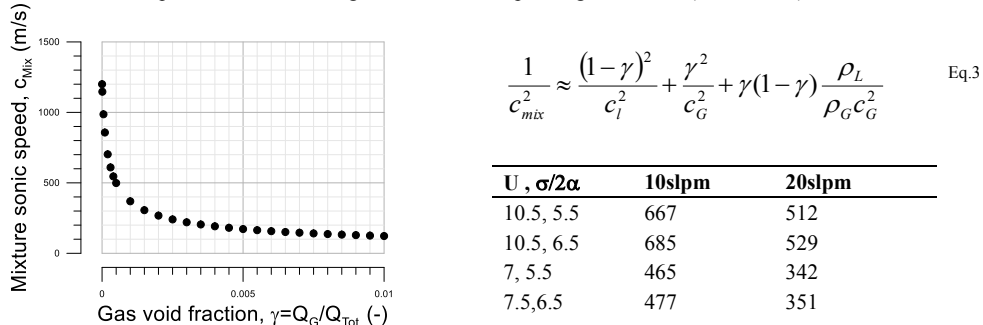


Figure 8: Mixture sonic speed.

Table 2: Calculated sonic speeds, c_{Mix} , in lower leg pipe for various air injection rates ($Q_{Gas,0}$) and operating conditions, $c_L=1200$ m/s

Results from modeling

Figure 9 shows the results for the pressure frequency response on the oscillating flow source. The latter is used to mimic the cavitation shedding action. The modeling has been used for one flow speed series, i.e. that of 10.5 m/s, and with various sonic speeds. Also included is the expected sonic speeds when injecting air at 20 slpm. Figure 9 also includes the measured pressure gain using the shedding load as the expected excitation. The calculations also include the pressure gain at the position of the hydrofoil, denoted p_0 .

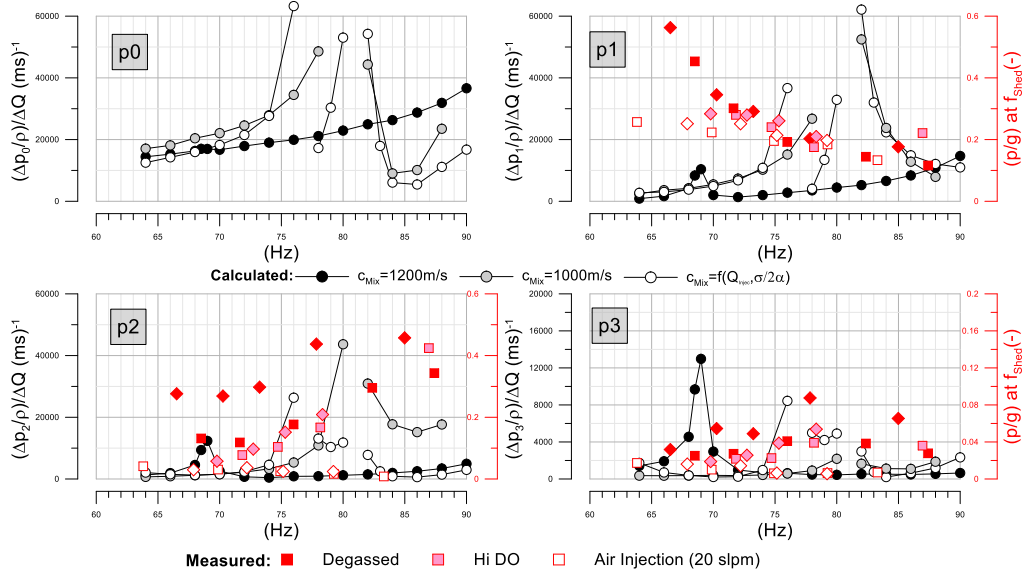


Figure 9: Calculated frequency response using the flow source as excitation, and measured pressure-dynamics gain relative to measured shedding load at shedding frequency. Calculations made for 10.5m/s and experiments presented for a test section velocity of 10.5 m/s (squares), and 10 m/s (diamonds)

Discussion

No direct modeling of the tunnel sonic speed exists, and thus the actual sonic speeds used during calculations remain uncertain. The use of continuous air injection should on the other hand affect the tunnel sonic speed to such a degree that any difference in facility dynamics due to sonic speed should be detectable.

Figure 9 compares calculated and measured response. The calculated response shows the presence of resonance peaks in the frequency range investigated. The measured response appears consistent, except for the offset in amplitude response for the two tunnel velocities at the p2 location and for the degassed tunnel quality. The observed response does not show similar tendencies of resonance conditions as the calculated response. The difference between calculated and measured or observed frequency response can be attributed to:

- A system amplified pressure oscillation at the position of the hydrofoil prevents a steady oscillatory condition since this requires $\sigma/2\alpha$, and hence the pressure, to be constant. Therefore, the true response for a given frequency will not be observed.
- For various reasons, free air can be trapped along the pipe loop. This will in effect lead to a multi-accumulator effect significantly altering system dynamics.
- As already mentioned the frequency dependency of the signal path between the hydrodynamic loads on the hydrofoil and the acceleration at the base is unknown, i.e. there is a chance that this unknown can obscure the readings in the frequency range tested.

While observing the frequency response for continuous air injection the dynamic response at the p2 and p3 locations is highly attenuated, while constant for the frequency range investigated in the p1 location. This suggests that the system acoustics is close to non-existing when injecting air into the tunnel. This observation supports the trapped gas argument.

Conclusion

The work presented suggests that cavitation shedding dynamics, quantified by shedding amplitudes and frequencies, is independent of tunnel water quality. The observed excitation loads as presented in Figure 4, support this conclusion. This study also indicates the presence of a systems response, both observed in Figure 6 and modelled and presented in Figure 9. Although the apparent negligible impact on excitation, the system response needs to be controlled and/or observed.

It is observed that continuous air injection attenuate system dynamics. At this point it must be emphasized the unique and efficient gas removal capabilities in the stilling tank of the SAFL water tunnel. I.e. the excitation, or hydrofoil cavitation shedding, is not affected by free air/ bubbles injected into the tunnel downstream the hydrofoil. Still, a conclusion from this work is the need for control and observation of pressure variations in the test section, this to cover the p0 dynamics depicted in Figure 9.

From a modeling perspective, an improvement can be made by modeling the interaction between the system and the hydrofoil cavitation shedding. For the case presented herein it can be achieved by coupling the transient 1D calculation with the 3D calculation of the hydrofoil cavitation. Also from an engineering perspective and for industrial application the interaction between the flow system and cavitation shedding interaction needs to be considered to avoid unfortunate combinations.

References

- [1] Lindgren, H. and Johnsson, C. A. (1966) "Cavitation inception on headforms, ITTC comparative experiments," Proceedings of the 11th Towing Tank Conference, Tokyo, pp. 219-232
- [2] Johnsson, C. A. (1969) "Cavitation inception on headforms, further tests," Proc. 12 Int. Towing Tank Conf. Rome, pp. 381-392
- [3] Keller, A. P. (1974) "Investigations concerning scale effects of the inception of cavitation," Proc. I. Mech. E. Conf. on Cavitation, pp. 109-117
- [4] Kjeldsen, M., Arndt, R. E. A., and Effertz, M. (2000) "Spectral Characteristics of Sheet/Cloud Cavitation," Journal of Fluids Engineering, vol. 122, no. 3, pp. 481-487
- [5] Kjeldsen, M. and Arndt, R. E. A. (2001) "Joint Time Frequency Analysis Techniques: A study of Transitional Dynamics in Sheet/Cloud Cavitation," in Fourth International Symposium on Cavitation (CAV 2001), California Institute of Technology, Pasadena, USA.
- [6] Arndt, R. E. A. (2012) "Cavitation research from an international perspective," IOP Conference Series: Earth and Environmental Science, vol. 15, no. 1,
- [7] Duttweiler, M. E., Schell, S. E., and Brennen, C. E. (2000) "The effect of experimental facility dynamics on a cavitation instability," in ASME 2000 Fluids Engineering Division Summer Meeting, Boston, Massachusetts, USA.
- [8] Kjeldsen, M., Vennaturo, R., Arndt, R. E. A., and Keller, A. P. (1999) "Discussion on cyclic cavitation in closed water tunnels and the influence from the dynamic response of the tunnel," in IAHR Work group on the behavior of hydraulic machinery under steady oscillatory conditions, Brno, Czech Republic.
- [9] Ekanger, J. V., Kjeldsen, M., Escaler, X., Kawakami, E., and Arndt, R. E. A. (2012) "Cavitation Intensity Measured on a NACA 0015 Hydrofoil with Various Gas Contents," in 8th International Symposium of Cavitation, Singapore.
- [10] Kjeldsen, M. and Arndt, R. E. A. (2009) "Blade load dynamics in cavitating and two phase flows," in 7th International Symposium on Cavitation, Ann Arbor, Michigan, USA.

Paper 4

Experimental assessment of pressure pulsations and transient characteristics of a 1400 m pipe line

I.K. Vilberg, M. Kjeldsen, B. Svingen, T.K. Nielsen

Published in Proceedings of the 13th International Conference on Pressure Surges, Bordeaux, France, November 14-16, 2018.

Experimental assessment of pressure pulsations and transient characteristics of a 1400 m pipe line

I.K. Vilberg^{1,2}, M. Kjeldsen¹, B. Svingen², T.K. Nielsen²

¹Flow Design Bureau AS.

²Norwegian University of Science and Technology, Department of Energy and Process Engineering.

This paper describes the initial experimental investigations carried out on a piping system with a total length of 1400 m with water at the test facility of the International Research Institute of Stavanger (IRIS). The test facility consists of two horizontal pipes with diameters 7" and 5.5", each with a length of approximately 700 meters connected with a 180° bend at one end. At the other end, the test set up included a pumping system attached to the 5.5" pipe, and arrangements for adding valves at the exit of the 7" pipe. The main objective of the initial testing was investigations of the wave propagation velocity in the system and the management of air content. Several tests were carried out with a rapid closure of a ball valve at the outlet to create a water hammer. Propagation of the resulting pressure wave was measured using pressure transducers at eight locations along the pipe and the flow rate was measured at the pipe inlet. Furthermore, a rotating disk was installed at the pipe outlet, causing a periodical variation of the outlet area of the pipe and thus imposing variation of flow rate and pressure. The pressure response of the system was measured using the pressure transducers. The experimental results were compared with analytical methods and simulations. The results revealed that air was still present in the pipe, even though several procedures were taken to minimize the air content. The fundamental frequency of the system of approximately 0.5 Hz was evident in both the water hammer and the oscillating flow experiments, which corresponds to the pressure wave being reflected before reaching the 180° bend. The measured pressure mode shapes show a $\frac{1}{4}$ wavelength for the fundamental frequency. However, the third harmonic mode shape with $\frac{3}{4}$ wavelength is found around 2.1 times the fundamental frequency for the measurements, whereas results from the simulations provides the third harmonic for 3 times the fundamental frequency as expected from theory. The results and experiences will be used as a foundation for further work and experimentation. A more comprehensive and improved experiment is planned to take place during autumn 2018.

1 INTRODUCTION

Design and operation of long pipe lines, typically found in oil and gas industries, water supply systems and hydro power conduits, require awareness of deleterious effects caused by pressure transients. Pressure transients arise from any change of flow rate, including start or stop of pumps or turbines and change in power demand in turbines (1). A severe pressure transient or water hammer due to a rapid closure of a valve, can cause pipe ruptures due to high pressure or cavitation damages and pipe collapse due to low pressure.

The test facility at IRIS (2) is an interesting site for experiments with pressure transients in industrial scale pipes. Several horizontal pipes of approximately 700 metres are a part of the full-size drilling test rig Ullrigg, as shown in Figure 1, and have previously been

used separately for testing drilling equipment and various valves, among others. The current study was initiated by Flow Design Bureau (FDB) and carried out in cooperation with researchers from the Norwegian University of Science and Technology (NTNU). For this experiment it was decided to connect the two horizontal pipes of 5.5" and 7" in one end to obtain a unique test facility of 1400 meters.

This experiment was initiated to assess the transient characteristics of the pipe loop and evaluate the possibility of further experiments on the test rig. In the current study, several water hammer tests were carried out to evaluate the wave propagation and the air content of the pipe. Furthermore, flow oscillations were imposed on the system by a rotating disk at the pipe outlet to create standing waves. The rotating disk valve was first introduced by Svingen for experiments on fluid-structure interaction (3). Tijsseling *et al.* have previously investigated unsteady friction in pipes with a similar rotating disk, both analytically (4) and experimentally on a smaller laboratory set-up with a 50 m pipeline with an inner diameter of 206 mm (5).

Experimental results from this study have been analysed and compared to simulations in the commercial software FloMASTER (6). The simulations assist in evaluating the presence and effect of trapped air. This experiment has served as a test run for a sequel experiment scheduled for October 2018, where flow control techniques will be applied to dampen the standing waves. The use of air injection to dampen pressure waves was also the topic for Vilberg's master thesis from 2010 (7).

2 EXPERIMENTAL SET-UP

The test facility consisted of two parallel horizontal pipes of 743 meters length connected in one end with a 180° bend connection. The pipe material was L80 steel, with inner diameters 154.8 mm for the 7" pipe and 124.3 mm for the 5.5" pipe. The surface roughness of the pipe wall was not measured. A pumping system was installed at the 5.5" pipe end and a valve on the 7" pipe end, at the "test site" shown in Figure 2. The water flow exited the pipe to atmosphere. The operational absolute pressure for the whole pipe-length was approximately 3 bars, implying a low flow rate with limited head-loss. Two smaller pumps were connected in parallel and supplied with water from a tank through flexible hoses. An accumulator consisting of a partly water filled vertical hose with an air pocket on top was installed downstream of the pumps to reduce possible pressure pulsations at the pump outlet. The flow rate of the system was measured by a flowmeter connected in front of the pipe inlet. Eight pressure sensors were mounted on pressure taps on the pipe, and the location is shown in Figure 2 and Figure 3. The 180° bend connection was located inside the IRIS yard, as can be seen in Figure 1. At this location it was possible to connect our pipe loop to the separate IRIS system pump, which was used for initial filling and flushing of the system.

A manual 1" ball valve was used at the outlet of the 7" pipe to impose a water hammer on the system. The valve was closed manually and faster than the reflection time of $T=2L/a$, where L is the pipe length and a is the wave speed. The propagation of the pressure wave was measured along the pipe. The second valve in use was a rotating Teflon disk with sinusoidal circumference which applied a periodical variation of the small slit outlet area of the pipe. A photo and 3d-model of the rotating valve is given in Figure 4. The Teflon disk had a diameter of 40 cm and amplitude variation of 2 cm with 1-4 sinus waves. The disk was driven by a motor to vary the slit area of 60mm x 16 mm with various

frequencies. The rotational speed was controlled by a frequency converter, resulting in an available frequency range of 0.1-60 Hz of the outlet area change of the pipe.

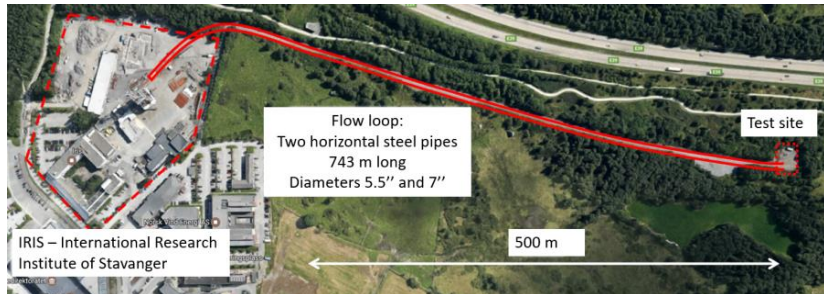


Figure 1: Overview of test site (8).

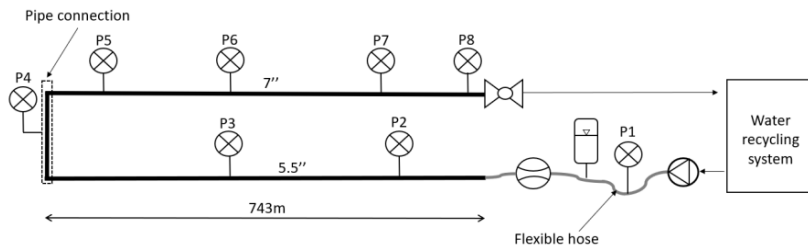


Figure 2: Schematic set-up of pipe experiment.

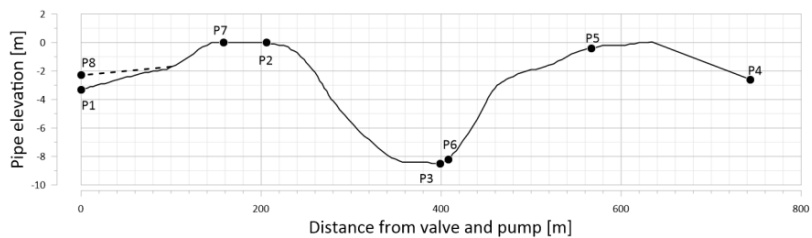


Figure 3: Pipe elevation and location of pressure sensors. 7" pipe elevated one meter above ground at valve location (dashed line).

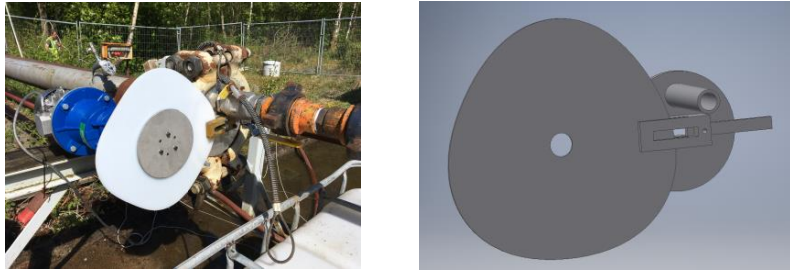


Figure 4: Photo and 3d-model of the rotating valve, with a circumferential variation of four and three sinus waves, respectively.

2.1 Signal recording

Signals were recorded using a National Instruments (NI) cDAQ 9188 chassis in combination with NI LabVIEW software. The pressure was measured with GE PTX 610 and Unik 5000 (PTX 5072-TB-A2-CA-H0-PA) with a range of 0-10 bar absolute and improved accuracy. The flow rate was measured by a Krohne Optiflux 4300 C EEX magnetic flowmeter (41-1500 l/min range, 0.2 % RDG accuracy). All data were recorded with a sampling rate of 1000 Hz using a NI 9205 module with a 499Ω resistance.

2.2 Simulations

The system was modelled in the commercial software FloMASTER (6). Figure 5 shows the IRIS pipe-line as modelled in the simulation software. The system is solved by applying the Method of Characteristics on the pipe elements. The rotating valve is modelled by applying a script solution, see Table 1. The script takes up- and downstream pressures together with the instantaneous valve opening as inputs, and calculates the flow rate, see lines 8 and 9 of the script. The pump characteristics for pumps (item 11 and 22 in Figure 5) were determined experimentally on site. The pipe wave speed for the 7" pipe is selected to be 1230 m/s which is considered a compromise for the experimentally determined wave speeds, see Figure 11. When comparing calculated with measured water hammer (WH) pressures, it was evident that trapped gas was present. An accumulator is therefore included to model this effect. The WH calculations were made with the accumulator in node 7 (bend) and in node 2 (close to the apex of the 7" pipe line) and as shown in Figure 5. Different stiffnesses (k') of the accumulators were tested. The relation being $\Delta p = k' \Delta h$ (bar), $k' = 1.4 (\rho_0/V_0)_{Gas}$, $\Delta h = \int q dt$, where q being the rate of change of liquid volume filling the air pocket. The better match of WH pressure signatures determined the accumulator size and location for steady oscillatory conditions. Figure 9 shows the result of this matching. The final accumulator chosen with values $\rho_0=2.44 \text{ kgm}^{-3}$ and $V_0=0.005 \text{ m}^3$ and a location close to the bend (node 7).

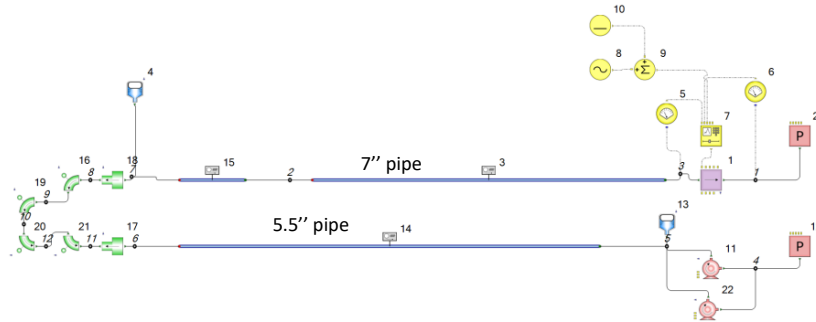


Figure 5: Graphical display of simulation model.

Table 1: Script applied to model the flow-rate through the rotating valve in the simulation.

1	If Manager.Time=0 Then
2	Controller.OutputValue=0.0
3	Else
4	p_us=Controller.InputValue(1)'From node (3)
5	p_ds=Controller.InputValue(2)'From node (1)
6	A=Controller.InputValue(3)'Mathematical construct elements 8, 9, 10
7	dp=p_us-p_ds
8	U=(dp/abs(dp))*(2*abs(dp)/1000.)^0.5
9	Q=A*U
10	If Q<0 Then
11	Q=0
12	Else
13	Q=Q
14	End If
15	Controller.OutputValue=Q
16	End IF

3 RESULTS

The pipe elevation varies with approximately 8.5 metres, as shown in Figure 3. Air was likely to be present at apexes of the pipe, thus repeated efforts of ventilation were carried out at those points. In addition to flushing the system with a high flow rate provided by the IRIS pump, several compression tests were conducted and the air content in the pipes was significantly reduced.

Results from the initial water hammer tests are shown in Figure 6-9, with an initial flow rate of 200 l/min, corresponding to a flow velocity of 0.17 m/s in the 7" pipe. The ball valve was closed manually, faster than the reflection time of the system to obtain a water hammer. The closing time was not measured. The results confirmed that a considerable amount of air was present in the pipes. The time series presented in Figure 6 show a high-frequency oscillation which is damped effectively due to the air content, in addition to a low frequency surge. The corresponding frequency spectra is shown in Figure 8. The same test was repeated after a procedure of reducing air content, and the

results can be seen in Figure 7 and Figure 9. It clearly demonstrates that efforts to reduce air content were successful. The fundamental frequency of approximately 0.5 Hz is clear in the frequency spectra.

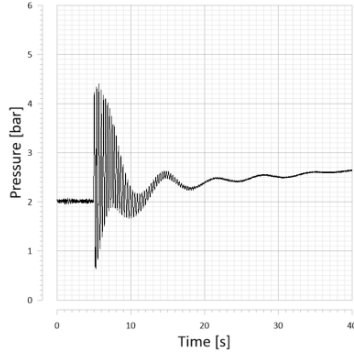


Figure 6: Time series of pressure at P8 before reducing air content.

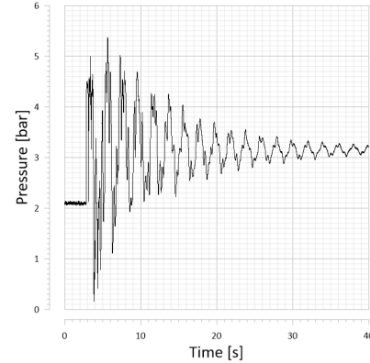


Figure 7: Time series of pressure at P8 after reducing air content.

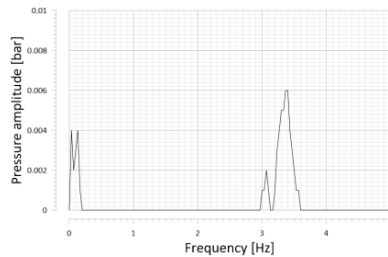


Figure 8: Spectral analysis of time series before reducing air content.

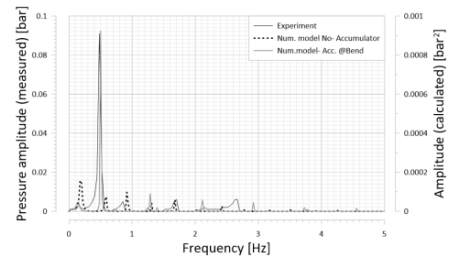


Figure 9: Spectral analysis of time series after reducing air content. Included results of calculated water-hammer solution with and without the accumulator.

The wave speed was evaluated by looking at the arrival time of the pressure wave at the different sensors along the pipe, as shown in Figure 10. Several water hammer tests were carried out. The flow rate was between 100-300 l/min for the measurements, which gave a flow velocity of 0.1-0.26 m/s in the 7" pipe. Arrival time has been identified for P8-P7, P7-P6 and P6-P5 to obtain an average wave speed. A weighted average of all results gave a wave speed of 1214 m/s. The largest variation of the measured wave speed was found between P6 and P5. The pressure wave was significantly damped before reaching the P4 sensor in the 180° bend and did not have a distinct pressure rise as the signals shown in Figure 10. Thus, results for the 5.5" pipe have not been considered further in this study.

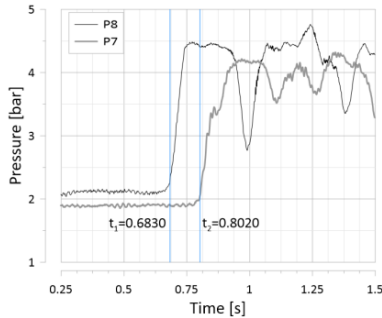


Figure 10: Evaluation of wave speed between pressure sensors.

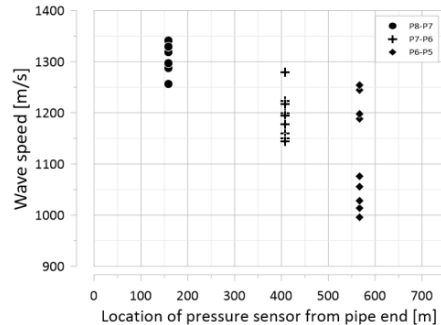


Figure 11: Measured values of wave speed between pressure sensors.

Following a series of water hammer experiments, tests were carried out on the valve with rotating disk. Figure 12 shows the amplitude of the pressure oscillations close to the rotating valve for a range of frequencies for the oscillatory flow experiments. The largest response of the pressure amplitudes was found around the fundamental frequency of approximately 0.5 Hz and the harmonic of approximately 2.2 times the fundamental frequency. Unfortunately, only scattered results were available for frequencies above 2 Hz and no further super harmonics can be identified.

Furthermore, the pressure amplitudes at the five sensor locations along the pipe is presented in Figure 13. The maximum and minimum pressure amplitude of the P8 sensor were located and averaged around ten milliseconds. Then, the pressure values at the other sensors at the same instant was found and presented graphically. A segment of the time series with steady oscillatory flow is also plotted for each pressure sensor to illustrate the pressure amplitude. The standing wave at the fundamental frequency has $\frac{1}{4}$ wavelength from the valve to the reflection point. It is evident that the harmonic of approximately 2 times the fundamental frequency is the third harmonic, with $\frac{3}{4}$ wavelength. However, results from simulations show that the third harmonic is 3 times the fundamental frequency, as shown in Figure 14, as expected from theoretical analysis.

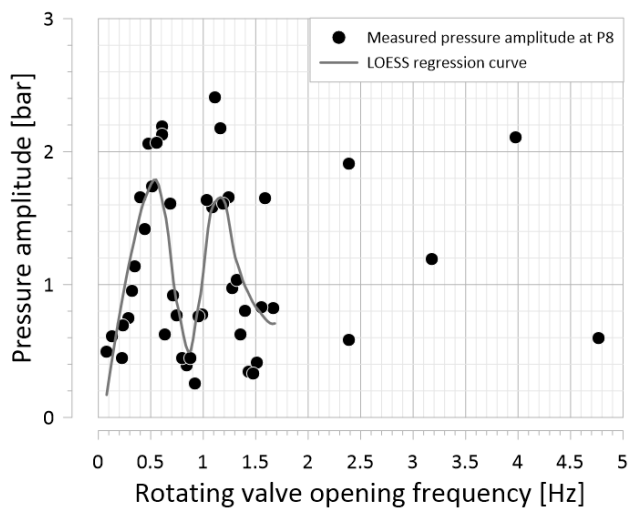


Figure 12: Pressure amplitude response on change of outlet area around the fundamental frequency.

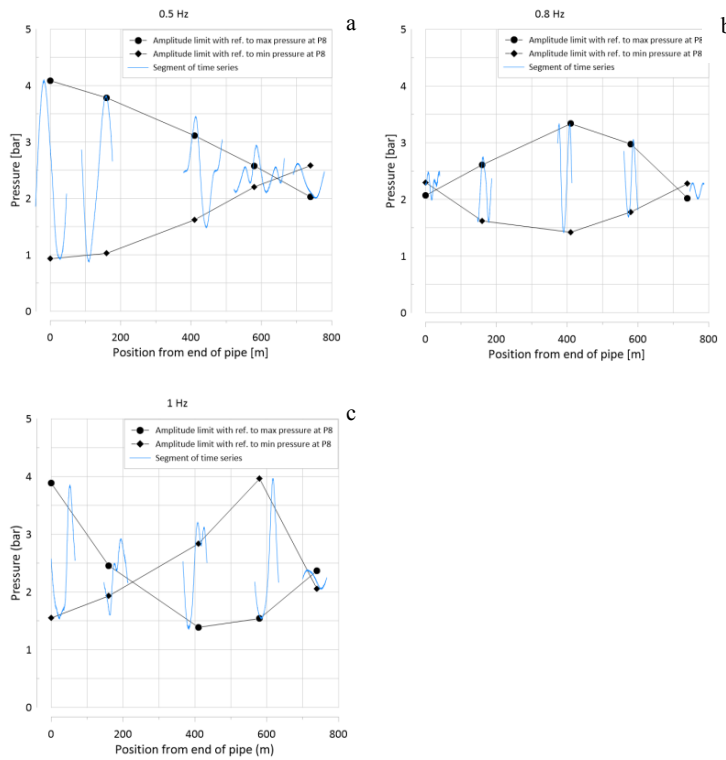


Figure 13: Measured pressure mode-shapes along the pipe for fundamental frequency 0.5 Hz (a), second harmonic (b) and third harmonic (c). A segment of the time series of the steady oscillatory flow at each pressure sensor is shown to illustrate the pressure amplitude.

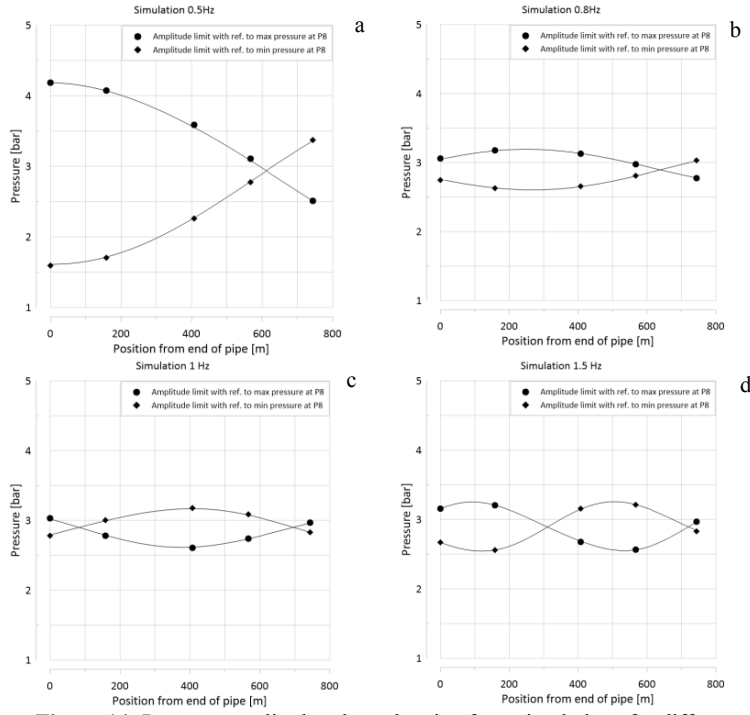


Figure 14: Pressure amplitudes along the pipe from simulations for different frequencies.

4 DISCUSSION

As expected, the air content of the pipe proved to be a challenge for this experiment. However, efforts to reduce the air content, i.e. ventilation at pipe apexes, flushing the system at a high flow rate and repeated compression tests, proved to be effective. Figure 6 - Figure 9 clearly demonstrate that the process of reducing air content in the system was successful. In the first test presented in Figure 6, the pressure wave is probably reflected at an air pocket close to the valve, and the pressure wave is quickly dampened due to a significant air content of the pipe. The results also show a low frequency mass oscillation in the system. The fundamental frequency of 0.5 Hz is clear in the water hammer experiments in Figure 7 after the air content is reduced. Using the equation for the theoretical period ($T=4L/a$) with a frequency of 0.5 Hz and a wave speed of 1214 m/s, the reflection length is approximately 607 m. This corresponds to the pipe apex around the location of the P5 sensor. By evaluating the wave speed as presented in Figure 10 and Figure 11 it was clear that the scatter in wave speed, especially between sensors P7-P6 and P6-P5, was not time dependent.

Results from the studies with the rotating valve also show the fundamental frequency of approximately 0.5 Hz. The fundamental frequency is $\frac{1}{4}$ of a wavelength in the pipe with

a pressure node at the reflection point and anti-node at the valve. The pressure amplitudes were increased around this frequency, and also around 2.1 times the fundamental frequency. This frequency was identified as the third harmonic in Figure 13, with $\frac{3}{4}$ of a wavelength in the pipe. According to theoretical analysis of ideal systems, the harmonics are odd multiples of the fundamental frequency like the results from the simulations given in Figure 14. However, for real and complex systems, the harmonics are not necessarily related to integers by the fundamental frequency. Even though the present study is on a straight pipe, it is far from ideal due to the air content and pipe transitions.

5 CONCLUSION

This work has shown the transient characteristics of the 1400 m long pipe loop at the IRIS facility and will be used as a foundation for further work and experimentation. A more comprehensive and improved experiment is planned to take place during autumn 2018. A procedure for reducing air content of the pipes have been established. The experiments revealed that the pressure wave was reflected before reaching the 180° pipe connection. Additionally, results from pressure sensors located on the 5.5" pipe show that the pressure wave was significantly damped before reaching the 5.5" pipe. Therefore, the next test will only use the 5.5" pipe as a supply pipe for the 7" pipe.

ACKNOWLEDGEMENTS

Master student Eirik Myrvold Hansen wrote his master thesis on this project, carrying out design of the rotating disk valve in addition to initial simulations and analysis. Olav Olsen provided invaluable guidance and help with all practical aspects of the experimental setup. The first author of this article, Ingrid K. Vilberg, is employed by FDB and enrolled as a PhD student at NTNU. FDB receives partial funding from the Research Council of Norway through the Industrial PhD Program.

REFERENCES

1. Wylie EB, Streeter VL. Fluid Transients in Systems: Prentice Hall, Inc.; 1993.
2. www.iris.no. Home page of International Research Institute of Stavanger (IRIS). (From 2019: <https://www.norceresearch.no/>)
3. Svingen B. Fluid Structure Interaction in Piping Systems: Norwegian University of Science and Technology; 1996.
4. Tijsseling AS, Hou Q, Svingen B, Bergant A. Acoustic Resonance in a Reservoir - Pipeline - Orifice System. CASA report 10-38; 2010.
5. Tijsseling AS, Hou Q, Svingen B, Bergant A. Acoustic Resonance experiments in a reservoir - pipeline - orifice system. Proceedings of the ASME 2013 Pressure Vessels & Piping Division Conference Paris, France 2013.
6. FloMASTER 8.1. Mentor Graphics.
7. Vilberg IK. Airbag for piping systems: Norwegian University of Science and Technology; 2010.
8. Hansen EM. Planning, start-up and testing of a pipe flow loop for the investigations of transient characteristics: Norwegian University of Science and Technology; 2017.